CIRP Annals - Manufacturing Technology 00 (2022) 1–24

Contents lists available at ScienceDirect

CIRP Annals - Manufacturing Technology

journal homepage: https://www.editorialmanager.com/CIRP/default.aspx

Mechanical interfaces in machine tools

Erhan Budak (1)[a,*], Atsushi Matsubara (1)[b], Alkan Donmez (2)[c], Jokin Munoa (1)[d]

[a] *Manufacturing Research Laboratory, Sabanci University, Orhanli, Tuzla, Istanbul 34956, Turkey*
[b] *Department of Micro Engineering, Kyoto University, Kyoto, Japan*
[c] *National Institute of Standards and Technology, Gaithersburg, MD, United States*
[d] *Dynamics & Control, Ideko, Elgoibar, Basque Country, Spain*

ARTICLE INFO

Article history:
Available online xxx

Keywords:
Machine tool
Structure
Mechanical interfaces

ABSTRACT

Machine tools involve various mechanical interfaces in different forms and styles, which affect performance significantly in terms of rigidity, thermal stability, precision, and accuracy. This paper reviews the state-of-the-art and future trends in machine tool structural interfaces. The main concepts, challenges, and improvements regarding mechanical and thermal characteristics, geometric accuracy and precision, and wear and failure of machine tool interfaces are presented. Advanced methods for modeling static, dynamic, thermal, and geometrical behavior of mechanical interfaces are presented with examples. Furthermore, typical wear and failure mechanisms and available solutions and health monitoring techniques are covered.

1. Introduction

Machine tools are assembled mechatronic systems composed of structural elements, drives, and their interfaces. This keynote reviews the research focused on mechanical interfaces in machine tool structures, allowing better understanding of recent trends and future needs in this area. A mechanical interface in a machine tool consists of two mating surfaces, which may or may not be of the same material, contacting or separated by another medium, such as lubricant, oil, or air. The function of an interface is to support the mating components of a joint while enabling its desired degree of freedom. The performance of the interfaces towards achieving their specific functions have significant influence on the overall machine tool performance. That is why extensive research has focused on machine tool interfaces. Machine tool designers and users should design and select interfaces considering their functional characteristics to optimize machines and processes. Component designers, in turn, should enhance the performance of interfaces considering their influence on the performance of machine tools. Improved performance of interfaces results in higher static and dynamic stiffness, precision and motion accuracy, thermal stability, and energy efficiency of machine tools.

Better understanding of machine tool interfaces enables the identification of the proper mathematical models in contact mechanics, providing accurate prediction of interface behavior at the component and assembly level from the early design to operation stage. It also enables performance improvement of the interface through the possibilities of lower friction, less heat generation, better precision and motion accuracy, and increased rigidity. In general, a better understanding of machine tool interfaces provides conceptual and practical advantages. The conceptual one is the accurate modeling of interfaces by considering mechanical, and thermal aspects. The practical one is designing and realizing the assembly considering accuracy, durability, life, and interface failure. A complete application of these concepts would certainly advance the system efficiency and complete product life cycle of machine tools. Furthermore, with increasing digitalization trends in manufacturing, digital twin has already become one of the major constituents of machine tool research and industry. Integration of machine tool interfaces for offline and online digital twin applications requires fast and accurate prediction of interface properties. The challenges to establish this link can be summarized as follows.

The first step to transferring or replicating the machine tool interfaces from the physical to the virtual domain is identifying the contact problem which requires distinguishing suitable mathematical models in contact mechanics with proper boundary conditions for interface behavior predictions and digital model updating on-the-fly. Modeling of machine tool interfaces needs integration of different mathematical models in contact mechanics. A complete mathematical contact model requires the evolution considering many aspects, such as integrating static, dynamic, and thermal parts of a contacting system into the model, which results in a complex and nonlinear model. Even a simple contact model without integration of different aspects exhibits high nonlinearity. Generally, one contact model theory predicts one variable by keeping other factors constant. Typically, this approach is insufficient to resemble the interface behavior in contact. So, one needs to use a combination of the contact models, which causes mixed boundary conditions. And these varied boundary conditions bring nonlinear effects from each other, resulting in evolving boundary conditions and entangled loops required during solution to capture these evolving boundary conditions. Apart from the interaction of different conditions, tribological parameters such as lubricants, wear particles, and scatters due to wear are the other reasons for evolving boundary conditions.

The second step to transferring or replicating the machine tool interfaces from the physical to the virtual domain is choosing

* Corresponding author.
E-mail address: ebudak@sabanciuniv.edu (E. Budak (1)).

https://doi.org/10.1016/j.cirp.2022.05.005

solution or iterative update algorithms of the contact problems for interface behavior predictions and updates. The employed procedures require careful selection of solution algorithms, which may suffer from convergence issues due to high nonlinearity. Several analytical and numerical methods are employed to predict the solution of contact problems in different components of the machine tools- that demonstrate considerably different interface characteristics- such as spindle bearing systems, feed drive and sliding components, spindle-holder-tool interfaces, and clamping systems.

The last step to transferring or replicating the machine tool interfaces from the physical to the virtual domain is the experimental procedure to identify and verify the contact parameters of machine tool interfaces. Measurement of mechanical interfaces requires precise and accurate experimental set-ups that are open to many problems.For instance, contact compliance measurement of a moving system requires a very large number of experiments which is often difficult or impossible to accomplish. Another example is thermal and accuracy investigations involving many sensors and measurement instruments.

Machine tools are most likely one of the most challenging engineering systems to design and model. Machine tool design focuses on the stiffness rather than the strength criterion. These criteria can be at odds with each other because typically a stiffer system has less damping and is more likely to be dynamically unstable. However, most other mechanical systems are designed according to the strength criterion, like an airplane wing or fuselage. Therefore, to achieve various performance and functional requirements during machine tool design, and since machine tools interfaces significantly affect system (or assembly) stiffness, categorization of machine tool interfaces is vital to find the most suitable solutions. In general, machine tool interfaces can be divided into three categories according to their mobility: static, quasi-static, and moving interfaces (see Figs. 1 and 2). Production of parts requires variation of relative position of different elements actuated by drives and supported by moving interfaces (see Fig. 1). The moving interfaces are critical factors for the accuracy and dynamic stiffness of a machine. Furthermore, friction in the moving interface is a fundamental obstacle to precision. During the last century, machine tool designers have tried to reduce friction to increase the accuracy of machines. This way, the metal-metal contact is avoided by introducing materials, systems, and lubricants with low friction such as hydro-static/dynamic guideways. Rolling elements were also included from the very beginning. In the last decades, new aerostatic and magnetic guideways without contact have been introduced for precision applications. On the other hand, friction is one of the most potent factors to suppress vibrations by damping the machine. Therefore, the quest for increased accuracy may yield a reduction in the dynamic stiffness of machine tools.

Due to economical and practical reasons, machine tools are not constructed from monolithic structures. Some parts of machine tools are joined through static interfaces (see Fig. 2) that do not change their relative position after the assembly. Bolted joints are the most widely used static interfaces to assemble different elements of the machines. Welding is also a widely used method to create static interfaces in machine tools. Glued parts are used as alternative solution in some cases. The compromise between precision and damping appears again with static interfaces. In general, high number of static interfaces increases the overall damping of a machine, but has the potential to increase alignment errors, and thus reduce accuracy.

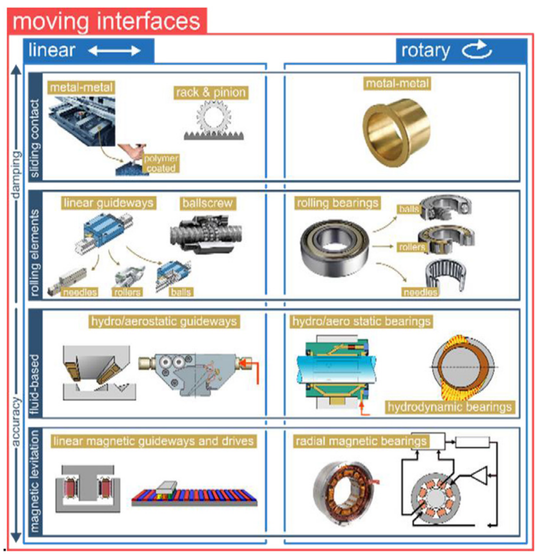

Fig. 1. Moving interfaces in machine tools.

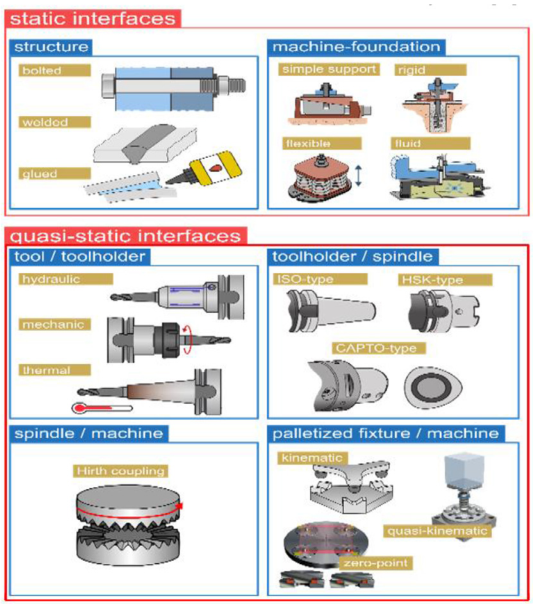

Fig. 2. Static and quasi-static interfaces.

Machine tools are flexible production units where tool, spindle head, and parts can be changed without losing the overall accuracy. The use of quasi-static interfaces permits automatic and accurate interchange of these elements. The connections between the tool and tool holder, and the tool holder and spindle have crucial importance in the cutting process and are highly standardized [1]. In heavy-duty and multitasking applications, the spindle heads could also be exchanged automatically, generating quasi-static interfaces. Similar interfaces are also used in palletized systems. The precision and accuracy of mechanical interface have a direct impact on the geometrical accuracy of the manufactured products. The accuracy of moving interfaces is improved by reducing the error motions of individual moving components themselves or the relative motions with respect to each other.

Properties of such interfaces and their characteristics, modeling, and methods to improve the total geometrical accuracy of such interfaces are discussed in detail in this keynote paper.

The paper is organized as follows: the existing literature is divided into four sections according to required conceptual and practical concepts for analysis, design, or selection of machine tool interfaces with a better understanding. In Section 2, mechanical characteristics of machine tool contacts are introduced and discussed by considering their static and dynamic behavior. Different contact mechanics perspectives such as tribology, applied mathematics and continuum mechanics are employed in machine tool research. Overall, the studies in those can be categorized into four main groups for determination of mechanical characteristics in machine tool contacts: (i) Analytical models, (ii) Numerical models, (iii) Experimental and identification methods, (iv) Hybrid models. Spindle bearings are the most studied among the machine tool components employing numerical and analytical methods for their contact properties. Likewise, the effect of the spindle bearing on tool point dynamics in idle and rotational states are studied by employing identification methods.

In Section 3, thermal aspects of machine tool contacts are presented by considering heat generation and heat conduction modeling and analyses at mechanical interfaces. In the first part, heat generation models in spindle and feed-drive systems are introduced. The models for thermal contact conductance and resistance at machine

Please cite this article as: E. Budak et al., Mechanical interfaces in machine tools, CIRP Annals - Manufacturing Technology (2022), https://doi.org/10.1016/j.cirp.2022.05.005

tools are introduced and discussed in the second part. Thermal contact compliance has a complex and hard-to-predict nature which causes many problems on stationary and moving machine tool interfaces. This situation requires an identification process and uncertainty analysis, which are also covered in the third section.

In Section 4, the geometric accuracy and precision of mechanical interfaces are discussed. Different machine tool interfaces are categorized mainly in three areas: static, quasi-static, and moving interfaces. These interfaces are covered in the corresponding subsections, where each interface's characteristics, modeling, and measurement methods are reviewed in detail. In addition, instruments employed to predict and evaluate the geometric accuracy of these interfaces and resulting motion errors are compared and discussed.

Equipment failure and decreasing productivity could arise from contact failures and defects. As a result, detecting a problem and identifying its position in contacts are essential for safe and reliable machinery operation. In Section 5, wear and failure types and defect categorization in contact interfaces are given, and methods for monitoring their health are discussed.

Finally, in Section 6, the discussions and conclusions are shared, while the future outlook for machine tool interfaces is discussed in Section 7.

2. Contact mechanics of mechanical interfaces in machine tools

Studies of contact mechanics establish the foundation for the research on machine tool mechanical interfaces. The contact mechanics perspective of tribology and continuum mechanics has offered different contact models. However, many of these models are limited to a few components with surface stresses. They do not allow predictions concerning plastic or more complicated failure mechanisms. Despite rapid development of various perspectives on contact mechanics in the last couple of decades, the unsolved nature of contact modeling attracts researchers from applied mechanics and machine tools. Some researchers have proposed experimental, identification, or hybrid models to overcome the mentioned problems since machine tool contacts are vital for precision and accuracy. Sections 2.1 and 2.2 examine mechanical models of machine tool contacts based on different perspectives. In Section 2.1, the tribology perspective for machine tools is introduced, whereas in Section 2.2, applied mathematics and continuum mechanics perspectives are presented. In Sections 2.3 and 2.4 models that use experimental and identification techniques and hybrid models are presented.

2.1. Analytical models

In tribology, contact problems can be classified according to various aspects such as the type of the material law, geometry of the applied load, contact configuration, friction and adhesion regime, or the shape of the contacting bodies. To give a general idea for machine tool contacts, analytical prediction methods are investigated according to the solution method of the contact problems which can be grouped in two categories: (i) Analytical (Exact) Methods and (ii) Semi-Analytical (Approximate) Methods.

Analytical solution methods

Hertz and Boussinesq provided the first exact solution for a particular contact problem class. The definition of the contact problem class was limited to frictionless and normal contacts for the geometries that can be reduced to 2D problems such as curved axisymmetric profiles or punch problems. These cases are classified as “Boussinesq problems” in the tribology literature [2]. Schubert (1942), Galin (1946), Shtaerman (1949) and Sneddon (1965) established the exact solution of these frictionless contact problems in their general form [3].

Semi-analytical solution methods

Semi-analytical approaches include numerical manipulation techniques to solve complex contact problems (multi-dimensional parameter spaces) by employing classical or benchmark analytical formulations. Using semi-analytical models is a must for frictional contact problems as they generally provide solutions for 3D complex contact geometries. In tribology, classes of frictional contact problems can be grouped as follows [2]:

- Mossakovski problems (normal contact with only sticking).
- Tangential problem (with slip and stick).
- Torsional contact.

Boussinesq and tangential problems (generally in Cattaneo−Mindlin form) [2] have applications in analyses of machine tool interfaces. Another important semi-analytical method is the fractal contact theory as it provides scale-independent asperity contact loads and assumes variable curvature radii in the contact analyses of rough surfaces for machine tool interfaces [4].

2.1.1. Static models

Among machine tool interfaces, spindle bearing modeling is one of the most-studied topics, and most of the related research uses analytical solutions provided by Hertz and Boussinesq. Even though the Hertz contact theory dates to the 1880s, the complete Hertz contact solution was completed in the 1960s. First, [5] introduced and popularized two degrees of freedom (DOF) (only axial and radial translations) models for angular contact bearings based on solutions of Hertz and Boussinesq, and provided a purely analytical solution by using Sjövall integrals. Subsequently, the analytical solution of five DOF angular contact bearing models (three translations dx, dy, dz and two rotary $d\theta_y$, $d\theta_z$) was provided by Houpert [6]. Two and five DOF bearing stiffness models, by considering contacts, were introduced by Hernot et al. [7] using them in specialized Finite Element (FE) libraries. After nearly two decades of obtaining complete solutions of Hertz and Boussinesq problems, Pruvot et al. [8] raised the first questions specifically for spindle bearing contacts by considering thermo-mechanical spindle behavior. Later, several parameters on bearing contacts were also considered. For instance, Jedrzejewski et al. [9] used a 2D simplified Hertzian model for modeling spindle angular bearings by considering centrifugal forces and gyroscopic moment. In high-speed spindle systems, enforcing for maximum possible contact area increases the radial stiffness. However, changing nature of the contact and thermal influences make this task difficult. To overcome this difficulty, Wock et al. [10] offered three- and four-contact-point spindle bearings to increase the contact area for high-speed spindles using analytical Hertz solution and an optimized Hertzian contact pressure profile to obtain constant operating conditions. Yuksel et al. [11] used the idea of enforcing for maximum possible contact area for early and quick prediction of thermal growth in spindles by separating contact penetration and sliding in a computer simulation. The preload change in bearings is obtained by employing an analytical Hertz solution.

Rolling element bearings constitute a statically indeterminate, nonlinear, elastic system. The related equations are not easily reducible to closed-form solutions despite many assumptions and simplifications [12]. Therefore, semi-analytical methods, which include linearized and iterative computation methods such as Newton-Raphson, graphics, and tables for rigorous treatment of bearing contacts, are offered in the literature to predict more complex bearing behavior based on classical Hertzian analysis [12,13]. Additionally, a five DOF (three translations: dx, dy, dz and two tilting angles $d\theta_y$, $d\theta_z$) bearing model and its semi-analytical solution based on both classical Hertzian analysis and modern Non-Hertzian contact analysis was presented by de Mul et al. [14]. Jones and de Mul bearing models are among of the first and most used semi-analytical bearing models in machine tool literature. In the classical model of Jones, the well-known nonlinear normal contact forces are given as the following (1),(2):

$$Q_0 = k_0 \delta_0^n \tag{1}$$

$$Q_i = k_i \delta_i^n \tag{2}$$

where δ_0 and δ_i are the deformations at points A and B, respectively, under the action of normal contact forces Q_0 and Q_i. The exponent n is called the load-deflection exponent. k_0 and k_i are the load-deflection constants at contact points A and B, respectively. These coefficients are dependent on the contact zone morphology and the contacting materials. The calculation methodology of load-deflection constant is presented in [6] for line and point contacts. Determination of contact angles and deformations (δ_0 and δ_i) requires iterative methods (generally Newton-Raphson) due to the observed high nonlinearity. For instance, [15] and [16] used iterative methods to predict contact angles and force deviations.

Another contact model for predicting the behavior of machine tool interfaces is the fractal contact theory. Since it applies to both Hertzian and non-Hertzian profiles, the fractal contact theory is used in analysis of various machine tool contacts from spindle bearings to machine tool joints. Since the rough surface profile (micro-asperities) can be represented by the Weierstrass-Mandelbrot function in the fractal theory, thermo-mechanical and dynamic behavior of bearing contacts can be modeled accurately compared to other methods. Therefore, the studies related to spindle bearings [17,18] generally include thermal and dynamic behavior prediction. To predict the contact stiffness at the machined joints, [19] employed the fractal contact theory. Another exciting application of fractal contact theory was exercised in [20] to represent concrete-steel joint interfaces in machine tools.

2.1.2. Dynamic models

One of the principal presences of contact dynamics is at the bearings. The dynamic models are usually developed based on the translational and rotational equations of motion of the ball relative to the bearing raceways and the interaction between the components in terms of total moments. Gupta proposed one of the distinguished analytical dynamic models for the ball and roller bearings' contact mechanism [21–24]. This model considers 3D motion of each bearing assembly component (inner ring, outer ring, ball, rotor) with six DOFs. This model provides the capability for the bearings with localized defects as well [25]. Authors in this paper updated Gupta's model by inserting the variation of deflections, Hertzian contact stiffness, and forces due to localized surface defects. The vibrations are evaluated and verified with experiments. Later, Niu et al. [26] used Gupta's model to investigate the cage whirl motions in ball bearings. In another work, the rolling ball bearing components (outer ring, inner ring, cage, and ball) are considered rigid body elements (RBE). Gupta's model is applied by including waviness, radial clearance, and pedestal effect. RBE discretization is also performed on the shaft and coupled with the bearing model to evaluate the vibration response of the bearing-rotor system by solving the dynamic equation of each RBE [27].

Another essential dynamic model for bearing stiffness calculation based on ball and roller contact with raceways is proposed by de Mul et al. [14]. This approach introduces an analytical model to calculate the Jacobian matrix of the bearing, which facilitates the computation of the the stiffness values easily without including gyroscopic moments. Based on this theory, Jorgensen et al. [28] modeled the dynamics of angular-contact bearings at high speed. By having both linear and angular bearing stiffness for a Hertzian spherical contact case, the vibration response of the spindle is predicted and verified. Later, this model was improved by Changqing and Qingyu [29] by developing a comprehensive Jacobian matrix for bearings considering centrifugal force, gyroscopic moment, and updated contact constants to study the effects of internal waviness and clearance.

Tlusty et al. [31] used an analytical approach to investigate the nonlinearities existing in the ball and roller bearings due to preloads. In another study, the nonlinearities in ball-to-race contacts are investigated to predict the bearing induced vibrations caused by the waviness of the rings and balls [32]. Chen and Hwang [33] proposed a quantitative analysis of bearing dynamics by introducing centrifugal force in Harris' model. The contact force and angle variations are analyzed at the ball/inner-raceway interface to determine the contact stiffness reduction at high speeds. In addition, contact mechanics at bearing/shaft and spindle/tool-holder interfaces are considered where natural frequency variations at high-speed conditions are studied.

In addition to contact issues in bearings and shaft interfaces, an analytical study is performed to investigate the contact stiffness variation of kinematic joints in a ball screw system at high accelerations [30] (see Fig. 3). The Hertz contact theory is used to determine the inertial contact forces for the dynamic model between screw-shaft and screw-nut interfaces. Hence, the equivalent stiffness of these joints is derived based on the contact state.

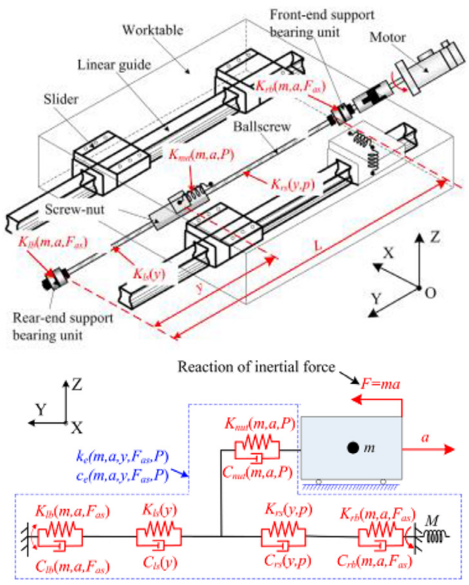

Fig. 3. The structure of a ball screw feed system and equivalent dynamic model of the ball screw feed system with high acceleration [30].

Dynamic stiffness modeling of machine tools based on machining space analysis is done by developing a stiffness synthesis model for an entire machine tool structure. This stiffness synthesis model combines the load transfer and deformation transfer matrices resulting in a low-order stiffness matrix model for the machine tool structure, verified by Finite Element Analysis (FEA) [34].

2.2. Numerical Models

In applied mathematics and continuum mechanics, contact phenomena are studied under the category of computational contact problems. The expression of a contact problem in computational contact mechanics dictates the impenetrability rule between the contacting elements [35].

The expression of the contact problem is known as Signorini's contact problem in the literature, and the impenetrability rule is denoted as the Hertz-Signorini-Moreau (HSM) conditions. The HSM rules (3) are expressed as follows [37]:

For all $A\epsilon\Omega_C^2$:

$$C_N u - g_u^\gamma \le 0, R_N \ge 0, R_N(C_N u - g_u^\gamma) = 0 \tag{3}$$

where $\boldsymbol{u}$ stands for the displacement field, and $\boldsymbol{C_N}$ is the transformation matrix of normal vectors on the potential contact surfaces. $\boldsymbol{g_u^\gamma}$ is a column vector which represents all gaps. According to Fig. 4, if the displacement is equal to the gap, a reaction force ($\boldsymbol{R_N}$) occurs due to the contact. This reaction force is zero if the displacement is smaller than the gap between the hitter and the foundation. In all cases the multiplication of the reaction force and the kinematic constraint will

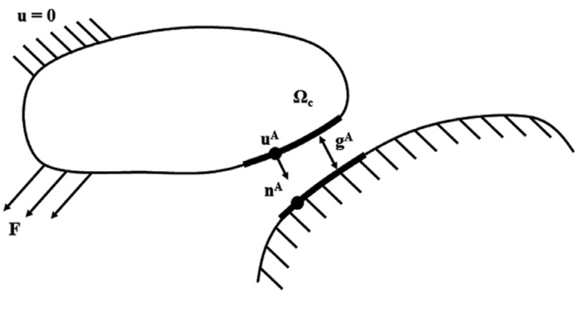

Fig. 4. The HSM conditions descriptive monograph [36,37].

be zero. Contact problems are expressed as optimization problems that minimize elastic energy while enforcing the HSM conditions. Therefore, the expression of contacts turns into nonlinear optimization problems for which the solution methodology is based on variational methods indicated in (4) where $\pi(u)$ stands for elastic energy, and $\boldsymbol{K}$ and $\boldsymbol{F}$ are assembly stiffness and force, respectively.

$$Min\pi(u) = 1/2\boldsymbol{u}^{\mathrm{T}}\boldsymbol{K}\boldsymbol{u} - \boldsymbol{F}^{\mathrm{T}}\boldsymbol{u},$$

$$\text{Subject to}: \; \boldsymbol{C}_N\boldsymbol{u} \le \boldsymbol{g}_u^{\gamma}, \; \boldsymbol{K}\boldsymbol{u} + \boldsymbol{C}_N^T\boldsymbol{R}_N = \boldsymbol{K} \tag{4}$$

Signorini's contact problem is fundamental for most computer-aided engineering (CAE) applications (finite element method (FEM), finite volume method (FVM), finite difference method (FDM), and multi body dynamics (MBD) with the only exception of the discrete element method (DEM). DEM uses semi-analytic methods and is also used in analysis of machine tool contacts [2,37].

2.2.1. Static models

Bearing or feed-drive contact modeling using FEM is relatively insufficient compared to those of hollow taper shank (HSK) tool holder-spindle interfaces because of the complex contact nature of bearings and feed-drives. Simplified HSK tool holder-spindle interfaces are generally modeled with FEM in machine tool literature since existing analytical methods are difficult to apply for such contact geometries that include Hertzian and punch contact profiles together. Researchers in [38,39] used different Finite Element (FE) software (MARC, Abaqus) to predict contact behavior. Other essential and inseparable Signorini's contact problem applications in machine tools are model order reduction and topology optimization. For instance, Law et al. [40] used classical FE-based penalty and multi-point contact formulation to couple already reduced substructures and topology optimization of a machine tool structure. Yuksel et al. explicitly demonstrated the difference between penalty contact formulation (FE-based) and spring representation of linear guides in topology optimization applications [41]. In the machine tool literature, this study is the first in dealing with machine tool contacts at the assembly level for topology optimization applications.

2.2.2. Dynamic models

FEM is a commonly used method for simulation and prediction of dynamic behavior in machine tool contacts. 2D FEM can be used to model the dynamics of rolling bearings with ring defects. Simple frictional contact is considered for all surface-to-surface contact interfaces of the bearing in [42].

In FE models for holistic simulation of machine tool dynamics, surface-to-surface contact, and node-to-face contact constraints are discussed. The conceptual idea is to distribute the forces and moments acting on the condensation node to the coupling nodes [44]. Full FE simulations are conducted on linear guide systems with the help of the component-oriented FEM in [43]. The contact mechanism between the ball and concave rails is replaced with two different equivalent models compared to the flexible ball contact theory. The first model considers rigid balls with equivalent material (RiBEM), as shown in Fig. 5, while the second one is Rolling Contact Spring (RoCS), consisting of a combination of nonlinear springs. Authors found out that both methods decrease the simulation time; however, due to the insufficient rolling contact representation in RoCS method, the induced error is significantly higher than RiBEM.

A coupled FE model of the machine tool frame and the spindle is performed in [45]. All components, i.e., spindle shaft, housing, cooling system, and machine tool frame, are modeled by the FEM. The stiffnesses of the spindle bearing system are calculated using Harris' model to analyze the dynamics of the whole system.

Despite time-consuming full FE models, Law et al. [40,46] proposed a position-dependent, sub-structurally synthesized reduced-order machine model to predict the dynamic response of the whole system. The multi-body dynamic model of a machine tool based on a reduced model provides less computational effort than the complete order FE models. Machine substructural components were reduced and

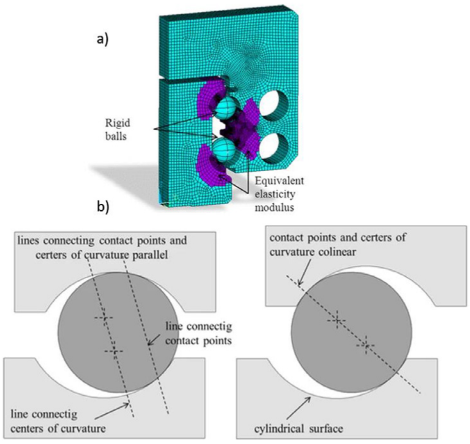

Fig. 5. a) Slice model of linear guide with rigid balls, b) Kinematic constraints of rigid rolling contact with friction (left) and frictionless (right) [43].

subsequently synthesized using adaptations of constraint equations that tolerate mesh incompatibility at their contacting interfaces, allowing for modular design. In another study, Zaeh et al. [47] combined the FEM and multi-body simulation of a system to simulate large movements in a machine tool. The dynamic response is evaluated by integrating nodal bodies in the multi-body system. This model is completed by considering the moving contacts on the flexible bodies.

Deng et al. [48] developed a FE model of the whole machine tool structure with different poses and spindle bearing dynamic parameters. The joint node dynamic parameters are modeled using spring-damper elements.

2.3. Models with experimental and identification techniques

All analytical and numerical methods have limitations in modeling of 3D complex machine tool interfaces with dry or wet working conditions. Additionally, rigorous treatment of machine tool contacts requires high computational power. Moreover, complex contact loading histories such as random vibrations acting on machine tools result in changes in dynamic contact properties that can potentially affect static contact properties in the long term. In machine tool literature, experimental methods are offered generally to extract contact parameters such as stiffness, displacement, and stress to deal with the issues mentioned above. Contact identification methods are presented to determine contact surface roughness or to extract a 3D map of contact interfaces. Both methods are widely used in machine tool research due to time advantage and application simplicity. Furthermore, contact parameter identification using experimental and analytical approaches were widely used in tool tip frequency response function prediction of the spindle-holder-tool assemblies. The dynamic contact models are used to identify the contact stiffness at tool-holder and holder-spindle interfaces using experimental measurement.

2.3.1. Static models

In the literature, experimental and identification methods are standard for the determination of machine tool contact characteristics. For spindles, [31] experimentally demonstrated spring behavior characteristics of spindle bearings with preload, lubricant type, and spindle speed change. Spindle stiffness measurement is a typical application, and there are mainly two methods for measuring the spindle stiffness: force-deflection method and natural frequency method. In this section, the focus is the force-deflection method. Zeljkovic et al. [49] offered a force-deflection-based stiffness measurement method. A novel non-contact stiffness measurement method was provided using a magnetic loading device [50]. Another stiffness measurement method that considers the softening and hardening characteristics of the machine tool spindle system was introduced by Li et al. [51]. Chen et al. [52] presented a practical method, which is an active bearing load monitoring and control mechanism that consists of integrated strain-gage load cells and piezoelectric actuators for bearing stiffness measurement and optimization. For tool holders, the interface behavior of different tool holders is examined and compared based on experiments [53]. Precise and accurate behavior of guideways depends on contact characteristics of guideway components, and material covers also affect the contact properties. Zatarian et al. [54] showed the effects of covering materials with experimental methods for contacts. Fan et al. [55] proposes a model with measured cutting forces and parameters of a slide-guideway. It can calculate the geometric errors of the slide due to contact deformation and the positioning errors caused by wear of the guideway after a long-term operation.

2.3.2. Dynamic models

Machine tool components frequently experience rolling, stick-slip, and skidding motion at wet and dry contact conditions, creating complex contact behavior that is hard to predict. To identify dynamic contact characteristics of such complex systems, experimental identification methods are developed. One can categorize these experimental and identification methods in three categories: modal parameter identification methods, physical damping identification methods, and friction identification methods.

Modal parameter identification methods

Modal parameters of an assembly may drastically depend on the contact conditions (contact stiffness and damping) at the contacting interfaces of substructures. Effect of interface contact parameters shows its significance at tool-holder-spindle assemblies. Stable cutting operation requires precise estimation of the frequency response function (FRF) at the tool tip. However, identification of the FRF for an arbitrary tool-holder-spindle assembly is time consuming which will increase the production cost. In order to overcome this drawback, Schmitz et al. [56,57] implemented the receptance coupling substructure analysis to predict the dynamic responses at the tool point by coupling the analytical or experimental FRF of each substructure to obtain the response of the whole assembly. This is performed by coupling the receptance matrices of each component which are evaluated analytically (see Fig. 6).

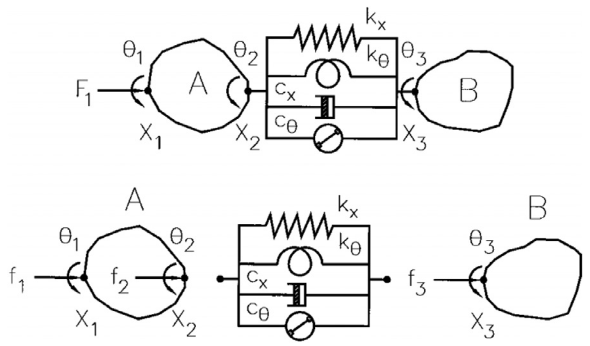

Fig. 6. Assembly and component systems in receptance coupling substructure analysis (RCSA) [56].

However, the identification of contact parameters at spindle-holder and holder-tool interfaces is the main difficulty.

Schmitz et al. [58,59] determine the contact mechanics at spindle-holder-tool interfaces by defining equivalent translational and rotational spring/damper between components. The values for springs and dampers were obtained by fitting the assembly RCSA and the experimental test. Namazi et al. [60] modeled the contact mechanism at the tool holder-spindle taper interface by using uniformly distributed translational and rotational springs. The stiffness values were obtained by error minimization method between the predicted and experimental measurements. Matthias et al. [61] identified the tool-holder contact parameters using fitting algorithm between analytical RCSA and experimentally-obtained tool point FRFs of the holder-tool assembly at free-free end conditions. Tool-holder interface contact modeling was enhanced in [62] by the multi-point receptance coupling method. In this approach, the contact length of the tool and holder are clamped at equally spaced points by employing flexible-damped coupling matrix. While Schmitz et al. [56] applied a lumped stiffness model through linear and rotational springs and dampers to the spindle-holder assembly, Movahhedy et al. [63] proposed a contact model with two parallel linear springs utilizing genetic algorithm. Schmitz et al. [64] extended the previous models with multi-point coupling for shrink fit holder-tool contact interfaces. An alternative approach was proposed by Ahmadi et al. [65] and Ahmadian et al. [66] instead of lumped-stiffness model. In these studies, the interface is considered as a layer where the contact pressure varies along with the interface. The previous approaches are based on the nonlinear least-square minimization between the predicted and measured FRF, which is time consuming in terms of practical applications. From different point of view, the contact properties at modular tools are investigated by Park et al. [67] using inverse receptance coupling method. Rezaei et al. [68] extended the inverse receptance coupling for several arbitrary point numbers in joint modeling. In the proposed approach the tool overhang is coupled with the subtraction of the analytical tool overhang FRF from the experimental FRF of the whole assembly which eliminates the need for identification of the contact stiffness/damping values by fitting method. In a different approach, Ozsahin et al. [69] used analytical receptance coupling method and tool point FRF results to identify the complex stiffness matrix, encompassing contact parameters for each frequency, and proposes a much faster algorithm for tool point FRF calculation. In this approach, the elastic receptance coupling equations for tool-holder-spindle assembly are rearranged by matrix inversion to obtain the complex stiffness matrices at each interface in a closed-form manner. Other researchers have used this method to obtain the contact parameters between the coupled structures [70,71]. Previously, Erturk et al. [72]proposed an analytical model to predict the tool point FRF of tool-holder-spindle assembly by combining the receptance coupling and structural modification technique [73] where all of the components are modeled using Timoshenko beam theory. The main components of the assembly were coupled by elastic receptance coupling technique by imposing the contact parameters at tool-holder and holder-spindle interfaces which are tuned experimentally by using FRF measurements. The proposed method was confirmed experimentally, and its use in accurate prediction of stability lobe diagrams was also demonstrated [74,75]. Erturk et al. [75] also showed that translational contact parameters (stiffness and damping) at the interfaces affect both frequencies and peak amplitudes of relevant modes of the structure significantly. This is also shown by Kivanç et al. [76] in structural prediction of end mills with different materials and geometries using receptance coupling method while the clamping parameters between tool and holder is studied and tool point FRF are predicted using receptance coupling method. The Timoshenko beam model is updated by Ozsahin et al. [77] by adding the effect of gyroscopic moments for rotor dynamic predictions. The bearing dynamics in idle state are also considered in identification of tool point FRF using receptance coupling method. The significant effect of spindle dynamics on tool point FRF under operating conditions are studied by Ozsahin et al [78]. The bearing dynamics are identified using inverse stability solution and in-process tap test [79] at high spindle speeds. The stability diagrams are modified based on the updated spindle dynamics. It is deduced that bearing stiffness and damping are affected by gyroscopic moments and cuttings forces as well as spindle speed under operational conditions which influences the tool point FRFs and hence, stability diagrams, drastically [80].

Damping identification methods

For physical damping identification of machine tool contacts, modal analysis based on impact tests are widely employed. Damping characteristics of a machine tool, and damper properties of viscoelastic support at its foundation are identified by impact tests in [81]. Another study to identify viscous damping parameters of a milling table with impact testing is done by Powałka and Okulik [82]. In [83], the vibration signal is acquired from the developed sensing system to identify the physical damping of the feed drive system with adjustable preload. The sensing system mainly includes the micro electro-mechanical sensor (MEMS) based detection and the signal processing circuit modules. The system has a small-sized detection unit so that it

Please cite this article as: E. Budak et al., Mechanical interfaces in machine tools, CIRP Annals - Manufacturing Technology (2022), https://doi.org/10.1016/j.cirp.2022.05.005

can be anchored onto the object of interest. Therefore, the preload variation can be reflected in the dynamic response of the ball within the ball nut. Another interesting viscous damping identification method is suggested in [84], which considers oil-film damping effects for rolling slideways. The main challenge in such a study is that several rollers in the slideways have various dynamic parameters for each in a rolling slideways system with damping oil films. Therefore, using pure analytical methods is challenging. Otherwise, that would lead to difficulty in studying the complex joint parameters. However, inserting oil- films in rolling slideways has similar characteristics with the study object of the modal modification method, which is also known as the receptance coupling method. This paper presents a model for the rolling slideways system with the damping oil-films by combining the receptance technique with testing data and avoids the analytical model of such a complex system.

Mounting elements are the static interfaces between foundation and machine tool, which support the machine tool's weight. Mounting elements also provide vibration isolation between the foundation and the machine [85], where passive supports are used in general [86]. Leveling block and jackscrews are the most popular mounting elements. Since there is a trade-off between stiffness and damping, these mounts may not provide sufficient damping. Therefore, research has investigated adding damping to passive mounts with sliding surfaces [87] or devising a coupling method [88]. The characteristics of the foundation itself also have a significant effect on the vibration characteristics of the machine tools. The influencing parameters include pile spacing, foundation thickness [89], surface treatment, and gravel layers [90]. The low-frequency vibration characteristics of the machine tool can be adjusted by the placement of the mount [91]. Although the mount is a static interface, it is affected by the aging of the foundation and requires periodic adjustment after the machine installation. To reduce the manual adjustment efforts, a mechanical adjustment method using mounting elements with embedded sensors, is proposed [92].

Friction models

Coulomb's friction model assumes that the friction force is opposite to the direction of velocity but independent of the magnitude of the speed. However, Stribeck discovered that friction decreases with rising velocity in specific velocity regimes by measuring the velocity dependence of friction in ball bearings. This phenomenon is called the Stribeck effect. Furthermore, stick-slip motion in machine tool components occurs frequently. As a result, these components experience pre-sliding motion, Stribeck effect during sliding, viscous damping, and hysteresis (due to structural damping). All these parameters affect the dynamic characteristics of machine tool interfaces. LuGre friction model successfully includes all the mentioned parameters with identification procedures. For instance, [93] identified all these parameters for a spindle head motion mechanism by employing the LuGre Friction model. Another study is conducted by Zhao et al. [94] for a feed-drive system again using the LuGre friction model.

Another friction identification method is the response surface methodology which is based on a series of experiments. The material, viscous, and structural damping of contacting machine tool bodies is investigated in [95] for cyclic tangential forces. The situations of various joint materials are compared. Predictive equations for damping in machined joints are developed based on experiments conducted on a rationale of economic data reduction through the response surface methodology (RSM).

Other than these categories, linear magnetic bearings provide a contactless medium for better dynamics and high accuracy at moderate cutting forces. Linear magnetic bearings can be employed in slideways, and dynamic characteristics of these systems are obtained by electrical current tests. In these applications, the measurement of bearing dynamic stiffness serves as an identification method of nonlinear system behavior that cannot be modeled off-line. The current tests for linear magnetic bearings provide this identification with the technique presented in [96].

2.4. Hybrid models

Experimental identification methods bring additional burden for designing and analyzing machine tools at the early design stage. One might employ pure analytical or numerical models to reduce costs, but pure analytical or numerical models also have some of the challenges described above.

There are different pitfalls for contact mechanics perspectives of tribology, applied mathematics, and continuum mechanics. One of the most challenging problems in all contact analysis is finding the complete stress tensors. Computational burden is another major challenge. On the other hand, the offered solutions in tribology do not allow predictions concerning plastic failure or more complicated failure mechanisms. In computational contact problems, the prediction of contact parameters is open to issues due to two main reasons. First, calculation of contact stiffness requires generally Newton-Raphson method due to nonlinear optimization problem given in Eq. (4). During the solution of FE process, the impenetrability rule of contact nodes by Hertz-Signorini-Moreau (HSM) conditions is satisfied by changing the contact stiffness which results in increased contact stiffness "erroneously" to avoid penetration of contacting node pairs. Second, the reliability of solutions varies according to the chosen computational contact method. These problems are explicitly indicated in a punch problem example by Yuksel et al. [36]. In Fig. 7, a flat punch problem is illustrated with FE results. In Fig. 8, the contact force deviation is illustrated for different FE-based contact algorithms together with an analytical solution.

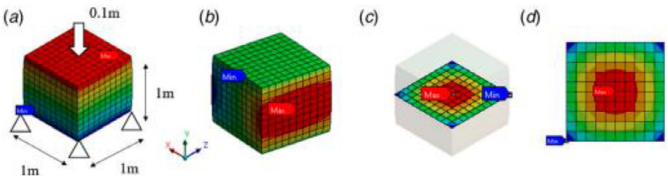

Fig. 7. The contact of half cubes: (a) the loading conditions and total deformation; (b) deformation at X-axis; (c) contact surface; and (d) oscillating contact pressure [36].

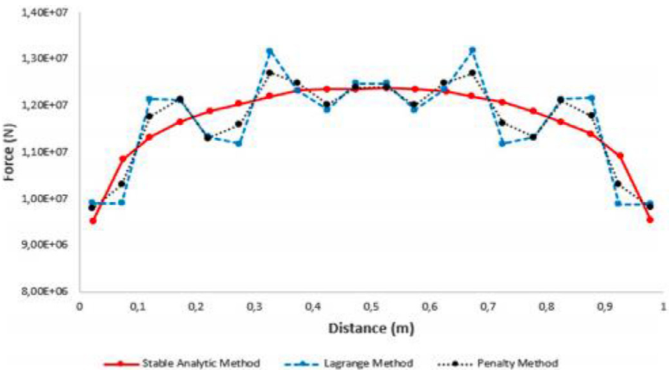

Fig. 8. Contact force variations for different computational methods in FE [36].

Therefore, hybrid contact models combining analytical and numerical representations are offered in machine tool literature to overcome the problems for machine tool contacts.

2.4.1. Static models

This section discusses models estimating static force induced deflections in contacts. Hybrid contact models used in spindles generally focus on thermo-mechanical behavior. The variation of contact angles and contact conduction properties of spindle bearing is modeled analytically in [97], and then representative FE models for the bearings are constructed during the simulations to predict thermo-mechanical spindle and preload behavior. Similarly, [98] presented a method based on the mechanical model of the bearing and the numerical model (FEM) of the spindle. The presented model includes a non-stationary change of temperature, thermal deformation, and bearing stiffness based on the angular position of the ball. Interfaces of spindle holders are experimentally identified and represented as virtual material inside an FE model [99]. For guideways, [100] considered tangential and normal contact properties assumed by employing semi-analytical contact prediction methods together. They created a virtual FE material based on the semi-analytical predictions (see Fig. 9).

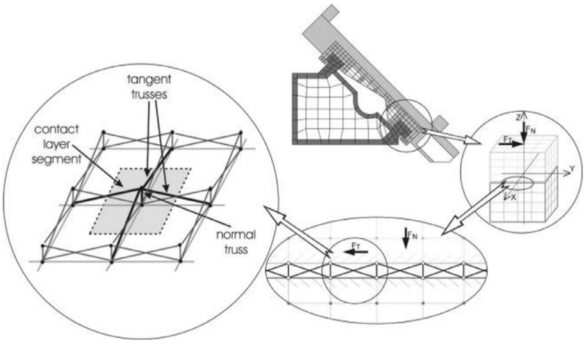

Fig. 9. Principle of modeling a contact layer in FEA [100].

For feed-drive system modeling, [101] defined a unique stiffness matrix to represent contact interfaces of feed-drive to use them in FEA. A hybrid FE model of screw-nut interface coupled with Timoshenko beam element having axial, torsional, and lateral dynamics is presented [102]. The screw-nut interface model is developed to capture both static and dynamic interaction between the axial, torsional, and lateral dynamics of ball screw drives.

Since finding complete stress tensors is impossible for machine tool contacts, generally equivalent stiffness models extracted from either experiments or analytical/semi-analytical methods are used in FEA to simulate machine tools at assembly levels. For instance, [103] proposed a methodology to assess the loaded conditions of individual joint errors in machine tools using an equivalent stiffness concept. The procedure is based on measuring the force–differentiation functions at the interface between the tool holder and table. The estimation procedure of the joint deviations is demonstrated in an analytical model based on a variational method and further implemented in a computational model describing the machine tool topology. Likewise, [104] presented a different equivalent stiffness approach that considers joint and leg compliances. Joints are modeled by a technological analysis focusing on the local behavior of the components for parallel kinematic machine tools. An equivalent contact force-based method called the reflected contact force method (RCFM) is proposed for FEA and topology optimization of machine tools [36]. The RCFM method maps experimental or analytically predicted contact forces to nodal forces at possible contact areas in the FE environment, resulting in accurate static and dynamic FE models. Since the RCFM maps contact forces to nodal ones, it is an efficient and superior vehicle for topology optimization. This study is the first in the machine tool field covering the multi-component topology optimization for machine tools by emphasizing the contact phenomena through the SIMP (Solid Isotropic Microstructure with Penalization) algorithm. This study aims to surpass and avoid the insufficiencies of the existing solution for the topology optimization of machine tool structures with contact constraints in FE software.

Chang et al. [105] used multi-body systems with transfer matrix and fractal interfaces for an ultra-precision machine tool and investigated the effect of bolted interfaces. The model simulation and experimental results show that the increase of the tool tip's vibration due to the 15% preload loosening at two joints was around 2, 3%.

2.4.2. Dynamic models

The studies using hybrid models can be classified into two categories which are discussed in the following.

Combination of transfer matrix and bearing models

A simplified approach for the transfer matrix method (TMM) considers bearings as rigid connection or linear spring-damper units in the roller bearing rotor system [106]. A coupled model of a high-speed spindle supported by angular-contact ball bearings is introduced using TMM and Jones-Harris bearing model to include the gyroscopic moments, which present benefits in the computation of the unbalanced response (see Fig. 10). The dynamic stiffness of the system is verified by experiments and used to predict spindle-draw-bar-bearing assembly dynamic behavior [107,108].

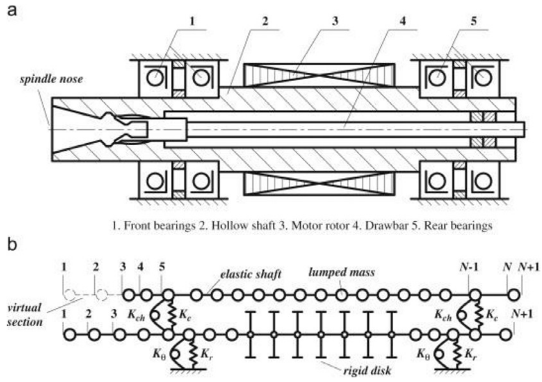

Fig.10. Spindle assembly model utilizing TMM[108].

Combination of FE and bearing models

Cao et al. [109] proposed a method to predict the dynamics of a spindle assembly by coupling the bearing model, spindle shaft, and housing. The nonlinear stiffness matrix for angular contact bearings is evaluated based on the Jones' model, the contact force between the ball and raceway is calculated based on Hertzian contact theory, while the shaft and housing were modeled as Timoshenko beam elements by considering the centrifugal forces and gyroscopic effects at both models. The contact forces, contact angles, and natural frequencies of bearings are studied under different preloads and rotational speeds. The results are used to determine the time history response and frequency response function of the spindle assembly under operational cutting forces. This model is updated in [110] by adding the effects of two bearing preload mechanism-"rigid" and "constant" mechanism and the dynamic behavior of the spindle system is analyzed in various rotational speeds. It is deduced that as the rotational speed increases the bearing contact/load decreases leading to low bearing stiffness and hence, low spindle rigidity at both preload mechanism. Brouwer et al. [111] employed Discrete Element method (DEM) for bearing dynamics model and FE for rotor modeling. The explicit FE model of the flexible shaft and the DEM model of bearings are coupled to transform the reaction forces and moments from bearings to rotor in all six DOFs of the of the bearing components. The ball-outer race way contact pressure was investigated at different speeds. It is seen that ball material affects the contact pressure and angle of the inner and outer raceways drastically, leading to change in bearing dynamics. In another similar approach, DEM, coupled with 3D explicit FE model of bearing cage, is used to predict the ball bearing dynamics in [112]. The contact interaction between FE mesh and the discrete bodies are explained with a novel contact algorithm. In this approach, DEM is used to calculate the contact force for a discrete element of ball and then distribute among the nodes at the vertices of the mesh element faces. Results show consistency with the classic Hertzian pressure distribution. A hybrid model of spindle dynamics was applied in [113] by combining the DEM model for floating displacement bearing and Gupta's angular contact ball bearing dynamic model with the FE model of the shaft based on the Timoshenko beam element. The shaft and bearings are coupled with forces and moments to transmit the vibration response at the installation nodes. Li et al. [114,115] combined de Mul's bearing and dynamic models of the shaft based on discrete lumped masses and thermal model to develop a comprehensive thermo-mechanical model of a spindle-bearing system. The contact stiffness at tool-holder-spindle interfaces is also included in the model.

Further studies are performed to analyze the dynamics of models of structures and implement the contact between components using FE models. For an accurate dynamic model of the structure, multipoint constraints connected to the spring-damper system represent the contact between the components of the machine tool structure. A coupled substructure model with consideration of local damping is presented. Four different approaches are discussed which allow coupling of substructures in arbitrary axis positions [116]. To avoid the computational cost, Irino et al. [117] introduced a method to comprehensively reflect the nonlinear dynamics of machine tool structures, including identified nonlinear stiffness and damping characteristics of linear guides, ball screws, and bearings using a magnetic shaker. The measurement-based method enabled a more realistic representation of the structural response of the machine tool that can be used to simulate the cutting process more accurately. The experimental results showed the improvement of the simulation accuracy.

Effects of components with linear guides on the vertical column-spindle system are studied using a hybrid model by FEM integrated with the contact stiffness model at the rolling interfaces. The role of the preload of the linear guide is investigated on the stiffness of the spindle head. The contact stiffness for bearings is calculated for FE using Hertz contact theory for the ball-screw contact where the manufacturer's data is used for the bearings [118].

3. Thermal aspects of machine tool interface

The management of heat generation and heat transfer is essential to avoid thermally-induced problems regarding accuracy and damage. The components and units of the machine tools have mechanical interfaces, and cause uncertainties in the thermal management. Since comprehensive topics on temperature modeling and thermal management were covered by past keynote papers [119,120], we focus here on problems including mechanical interfaces. Sections 3.1 and 3.2 introduce heat generation and heat conduction modeling at mechanical contacts, and then Section 3.3 presents thermal issues associated with mechanical interfaces.

3.1. Heat generation at mechanical interfaces

3.1.1. Heat generation in spindle

The major heat sources in the spindles are bearings and motors. Here, we focus on the heat generation of rolling bearings with mechanical contacts, which has been analyzed with modeling. The major models are explained below.

Palmgren-Harris model

The most known classic model for heat generation in spindle bearings is the Palmgren-Harris model (PH model) [5,121]. The model calculates generated heat, H, using the frictional moment M and the number of spindle revolutions n as follows:

$$H = 1.047 \times 10^{-4} nM \tag{5}$$

$$M = M_l + M_v + M_s \tag{6}$$

where, M_l, M_v, and M_s represent load-related, viscosity-related, and spin-related moments, respectively. When the rolling element rotates on the races with deformation, rolling and skidding motion occurs, creating spin motion. Harris explained the nature of spin and the calculation method of spin moment [121]. Jorgensen and Shin showed the calculation procedure of generated heat using Harris's formulas [122]. Jin et al. proposed more detailed spin moment calculations, where the contact radii are calculated from the load distribution of balls [123]. The PH model is given from numerous experimental data but includes uncertainty. The uncertainty is discussed by Kauschinger and Schroeder [124].

Elastohydrodynamic lubrication model

The contact pressure between the ball and the raceway of the bearing deforms the contact surfaces. High contact pressure increases elastic deformation and the viscosity of the lubricant. Fluid-film lubrication enhanced by hydrodynamic action is called elastohydrodynamic lubrication (EHL) [125]. The critical quantity in the lubrication is the oil film thickness, which is uniform in the large area of the contact region. The pressure distribution is almost the same as the Hertz pressure distribution except for a sharp peak on the outlet side due to the film thickness constriction. This causes the pressure center to shift to the inlet side and a traction force (rolling traction) even in the pure rolling state. In addition, the relative velocity generates slip traction force, which accounts for a large proportion of the friction torque of the bearing. The film thickness and pressure are obtained by solving the Reynolds equation numerically. The curve fit gives closed-form equations for the condition parameters. Houpert showed equations that express the traction forces with dominant parameters [126,127]. For example, the rolling traction force used in a point contact in the EHL regime is formulated as:

$$R_{EHL} = 2.86.E.R_x^2.k^{0.35}.U^{0.66}W^{0.467}.G^{0.022} \tag{7}$$

where U, W, and G are dimensionless quantities related to velocity, load, and contact surface material. E is the equivalent Young's modulus, k is the radii ratio, and R_x is the equivalent radius of the contact. Balan et al. applied this rolling traction calculation to a 3-ball thrust bearing and showed the results of experimental verification [128]. Testing and experimental verification of the Houpert model has been performed at Czech Technical University (CTU) in Prague, Research Center for Manufacturing Technology (RCMT), using an experimental test rig, shown in Fig. 11 (a). For the calculation of friction torque, a closed-loop thermo-mechanical simulation model was used [129]. The measured and simulated torque is shown in Fig. 11 (b). The continuous red line depicts friction torque calculated by the Houpert model with a bearing temperature fixed at 40°C. The green line shows the calculation for a single bearing considering the measured bearing temperature. The simulated torque matched the measured friction torque (black dotted line) over the spindle speed of approximately 8000 rpm by considering an actual bearing temperature. The light blue line is the result of coupled-models simulation, which will be explained in Section 3.3.1.

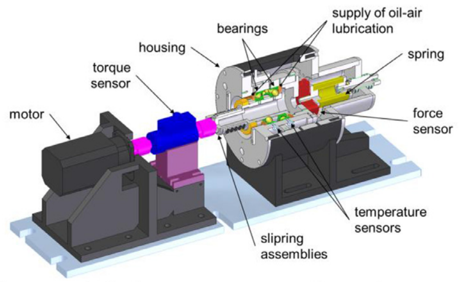

(a) Test rig (preloading system: spring, internal bearing diameter: 70 mm, lubrication type: grease or oil air).

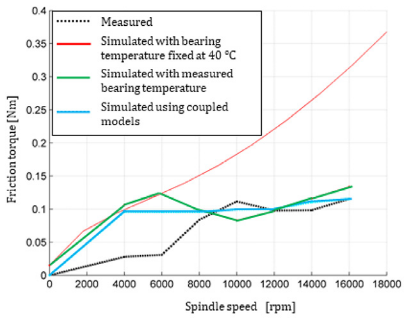

(b) Simulated and measured friction torque

Fig. 11. Bearing torque test rig and comparison of the simulation and experiment (by courtesy of the RCMT, CTU).

Other models

Brecher et al. calculated the cage friction, showing the significant impact on bearing heat generation [130]. EHL friction between the balls and the cage was calculated [131]. Bossmanns and Tu proposed a quick stop test to measure the friction named "coast test" and formulated an experimental model which can accommodate preload change [132]. With the development of computational mechanics, more detailed models have been studied. Gupta shows the numerical calculation method of traction from the arrangement of balls and orbit, by integration using the moving heat source [133]. This model is implemented in a bearing calculation software called Adore.

3.1.2. Heat generation in feed drive System

Ball-screw and linear-motor drives are mainly employed in modern machine tools. Typical models that represent heat generation mechanisms at mechanical interfaces have been investigated in the ball screw units and guideways.

Ball screw unit

A ball screw unit has moving contacts in the nut and the support bearing unit, which generate heat. In the support bearing, the heat generation was predicted using the PH model [134]. The heat generation in the nut is governed by the rolling and sliding friction of the rolling element. The contact relationship between the rolling element and the raceway groove at the nut is more complicated due to the lead angle. The preload is an important factor that dominates stiffness and generates drag torque dependent on the speed [135]. In many studies, the heat generation of the nut is also calculated using the PH model [136], where the preload is considered in the load-related term in (6).

Jedrzejewski et al. calculated the heat generation of the ball screw, where the preload change due to external forces (gravity force, inertial force) are modeled with a simple equation, which makes the estimation available during motion cycles [137]. Oyanguren et al. combined the FEM model of ball screw nuts and a shaft with an nonlinear stiffness model of the ball for calculating the prelaod [138]. The EHL model was also applied to the friction modeling of the ball screw [139].

Guideway

For guideways, many friction models have been proposed that consider the effect on motion and positioning accuracy. The amount of heat generation can be predicted by multiplying the frictions by the relative velocity of the contact surface. The simplest models are the Coulomb friction and the viscous friction models. For example, in the slide guideway, the frictional force and generated heat are estimated considering the surface pressure, viscosity coefficient, friction coefficient, oil film thickness, etc. [140].

Due to its wide velocity range at the moving interface of the guideway, boundary lubrication, mixed lubrication, and fluid lubrication are to be considered for heat generation. Cheng et al. proposed a precise model for the calculation of heat generation in linear roller guideways [141], incorporating the Coulomb friction and viscous friction with the Stribeck effect. The heat partitioning factor was defined and identified experimentally to divide the heat flow into blocks and rails.

3.2. Thermal resistance at mechanical interface

The heat transfer characteristics when two surfaces come into nominal contact are represented as follows using thermal contact conductance h_c (TCC), the reciprocal of thermal contact resistance (TCR).

(a) Complete insulation: $h_c = 0$
(b) Complete contact: h_c = infinite
(c) Contact with heat flux: h_c =constant, or variable

The range of h_c in the elements of machine tools are summarized in Attia's literature [142]. In the case of continuum materials, h_c is given in a simple equation by a thermal transfer coefficient and geometrical parameters. However, the contact surface causes the restriction of heat flux, which makes it difficult to give a closed form solution.

In Hertz contact, the contact resistance under mixed boundary condition between the ball and the ring [143] is calculated as:

$$R = \frac{\Psi(a/b)}{4ka} \tag{8}$$

where Ψ is the complete elliptic integral of the first kind, k is the thermal conductivity of the half-space, a and b are the semi-major and minor axes of the elliptical contact area. The model is used in TCC in the ball bearings [144,145].

Compared to such non-conformal contact, conformal contacts are dominated by the surface asperity of the real contact area. Scientific attempts to find the exact TCC for a nominal mechanical joint have been made for a long time [146]. Heat transfer through the interfaces formed by the mechanical contact of two solids occurs in three forms: conduction through the contacting spots, conduction through the gas-filled gap, and radiation. However, when the transmitting medium is a liquid or a solid, the amount of heat transferred by radiation is often negligible.

Fig. 12 illustrates the temperature change and heat fluxes of a boundary zone of two contacting materials. There are true contact spots and uncontacted areas on the nominally contacting surfaces, through which heat transmission occurs. The thermal contact conductance h_c is extended to cover the heat flux through the gas and defined by the sum of the contact spot conductance h_s and the gap conductance h_g :

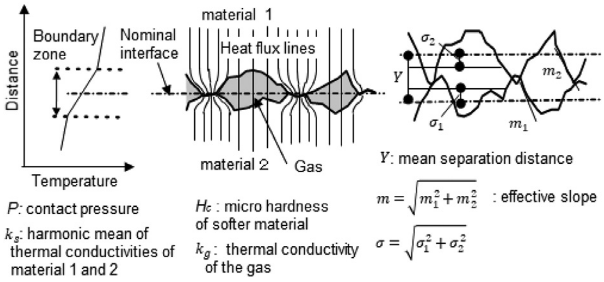

Fig. 12. Heat transfer at contact area with two surfaces

$$h_c = h_s + h_g \tag{9}$$

where h_s is influenced by the various contact conditions: contact pressure, material properties of contacting bulk materials, geometrical properties of contacting surfaces. The geometric-mechanical-thermal model was proposed in 1969 and is called the Cooper−Mikic−Yovanovich (CMY) model, which expressed TCC as shown in the following equation [147]:

$$h_s = a_1 \frac{k_s m}{\sigma}, \left(\frac{P}{H_c}\right)^{b_1} \tag{10}$$

where, $a_1$and b are the constants, which were given from the theoretical calculations and the experiments, shown in Table 1.

Table 1
Parameters for CMY model

Name	Refs.	a_1	b_1
CMY	[147]	1.45	0.985
Mikic	[148]	1.13	0.94
Yovanovich	[149]	1.25	0.95

P/H_c is the relative pressure of the contact surface, and its explicit version is seen in [150]. h_g is calculated by the following equation.

$$h_g = \frac{k_g f_g}{Y + M} \tag{11}$$

$k_g$is the thermal conductivity of the gas. M is the gas parameter, representing rarefied gas phenomena. f_g is a correction function with $Y/\ \sigma$ and $M/\ \sigma$, which avoids the underprediction. $Y/\ \sigma$ is calculated by the correlation of P/H_c [151]. If $f_g = 1$, $M = 0$ in (11),the gap conductance could be simply understood by the gas conductivity divided by the gap distance. This form is used for a simple estimation.

Jiang and Zheng used fractal theory on the contact surface to calculate the restriction of heat flux. They used the Weierstrass-Mandelbrot function to calculate the true contact area of the contact surface and explained that the fractal parameters could tell the range of the exponent b_1 [152] in Eq. (10).

3.3. Thermal issues including in mechanical interfaces

3.3.1. Static interfaces

Jedrzejewski proposed a practical TCC model, which combines a CMY representation and gap factors and takes the waviness and roughness of the contacting surfaces into account. The model was used to calculate the effect of layer thickness on the thermal resistance in the shaft−bearing−housing assembly for different materials [153]. Kim included this model for a thermal network model represented by a bond graph to estimate the stability problem in a spindle-bearing system [154]. Uhlmann and Hu developed a holistic 3D FEM thermal model of a high-speed cutting (HSC) machining center to estimate the distribution of temperature (see Fig. 13) and thermal deformation [155].

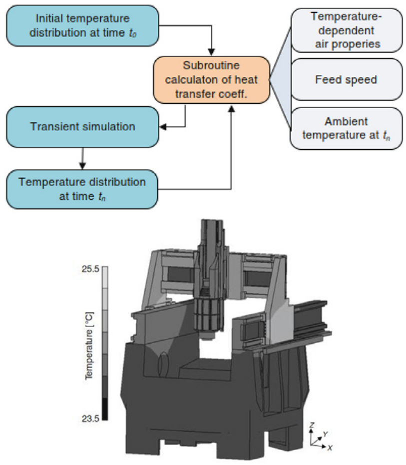

Fig. 13. Simulation for temperature distribution including heat transfer characteristics [155].

The model considered heat generated by linear motors and guideways, convection with ambient air, and TCCs between the component joints. For the estimation of TCC, Yovanovich's model was used assuming the pressure of bolted joints. For another representation of TCC, the fractal model was used for thermal deformation simulation of the spindle and the machine tool, where the difference with and without TCC has been reported [18,156−158].

Closed-loop interaction, in which thermal deformation changes contact pressure and TCC and promotes thermal deformation has been studied for a long time [159]. Attia and Kops simplified the CMY model, assuming that the TCC is linear to the contact pressure. Using the FDM incorporating a nonlinear model for the surface approach by the contact pressure, the iterative flow to determine the thermal deformation of the structure was proposed [160]. The combined effect of normal and shear contact stiffness on the thermal deformation was shown [161]. Closed-loop interaction is critical in spindle design. Holkup et al. built a FE model of a spindle with a shaft, bearings, and housing for the prediction of radial stiffness, considering TCCs between those components. They presented the importance of radial clearance and preload in the bearing assembly in both the simulation and experiment [129]. Returning to the discussion of friction calculation in Section 3.1.1, the light blue line in Fig. 11(b) shows the calculated friction torque using the same strategy. The computed torque agrees with the measured torque, which indicates the importance of considering a spindle structure's temperature and mechanical fields together with bearing kinematics and mechanics. Rabréau et al. reported that different ball-bearing kinematic hypotheses lead to noticeable variation in the bearing internal state (contact angles, stiffness), but the impact on friction torque calculation was relatively negligible [162]. They also showed that the effect of the axial force (preload) on the bearing state and stiffness was significant. It seems rather challenging to find force and temperature equilibria, where heat generation due to spindle friction is not large.

3.3.2. Moving interfaces

Compared to the spindle, a feed table moves in a wide range, and heat generation TCC changes from time to time. In addition, the feed drives are greatly affected by the convection with the environment, which complicates the prediction of the temperature distribution. With a simple TCC model and measured load, thermal deformation of the feed system was predicted for the moving interface in the ball screw [163,164]. For practical estimation, the generated heat was estimated by counting the number of times the nut moves along the screw [165]. For solving realistic thermo-elastic problems in actual operating states, Oyanguren et al. proposed a multi-physics analysis with more precise contact states, as shown in Fig. 14. They coupled a thermal field and stress field to calculate an induced preload variation [138].

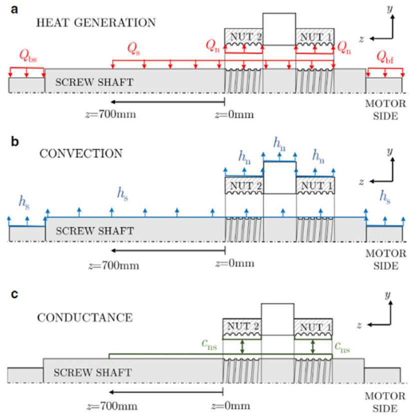

Fig. 14. Contact state change in ball screw [138].

Jedrzejewski constructed a holistic thermal deformation model for the turning center. The power loss of the ball screw in the Z- and X-axis operation cycles and the positioning error were estimated from the temperature change and elongation of the shaft using FEA [166].

3.3.3. Identification and uncertainty analysis

Various attempts have been made for thermal compensation by predicting thermal deformation [119]. One of the drawbacks is how to deal with the modeling uncertainties of heat generation, TCC, heat convection, and radiation. The measurement of temperature with an infrared (IR) camera together with contact pressure allows the identification of TCC in practical fields without a vacuum chamber [167]. Konvicka et al. used IR camera measurement for a modular tooling system to include radiation and convection percentage to the calculated heat-transmission coefficient [168]. Neugebauer et al. showed how to adapt the heat transmission coefficient of convection using distributed temperature sensors [169].

To obtain the accuracy and speed required for real-time compensation, methods for adjusting uncertain parameters considering their sensitivity have been proposed [170]. Ihlenfeldt et al. analyzed the sensitivity of heat generation and conductance to the temperature field using a thermal network model [171]. The accuracy of predicting temperature deviation was improved by identifying parameters shown in Fig. 15.

Uncertainties of heat input and TCC at the nodes increased the calculation cost in analyzing a large-scale model. Attention has been drawn to model order reduction (MOR), which can give compact and precise models for thermal analysis. Hernández-Becerro et al. applied Krylov modal subspace reduction to FE models and evaluated the influence of heat transfer coefficients on the thermal deviation of the tool center point [172,173].

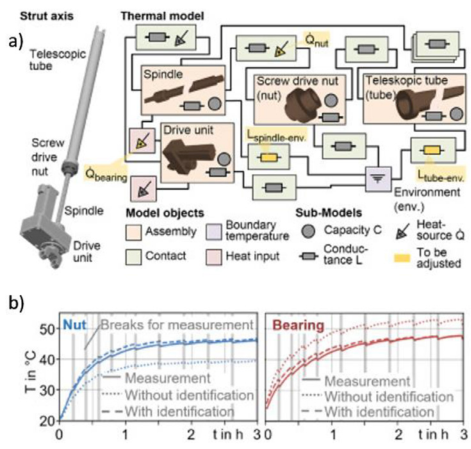

Fig. 15. Thermal network model and simulated temperature (a) schematic presentation of a thermal network model (b) Simulated temperature from models with and without identification [171].

4. Geometric accuracy and precision of mechanical interfaces

Machine tool interfaces determine the relative position and orientation between machine tool components. By properly distributing and transmitting the forces and torques, these interfaces also contribute towards the performance characteristics of the associated machine tool functions (e.g., motions of the cutting tool and the workpiece).

Machine tool interfaces are classified as static, quasi-static, and moving interfaces. Since in conventional machine tools, material removal is accomplished by the relative motion between the cutting tool and the workpiece, quasi-static and moving interfaces serve as the critical enablers for this function.

In the following subsections, the characteristics, modeling and measurement methods and instruments used for predicting and checking the geometric accuracy of these interfaces and resulting error motions are described.

4.1. Static interfaces

Static interfaces, which ensure no relative motion between the two mating faces, in general consist of welded or bolted joints connecting various machine tool structural components such as spindle head or rotary table to machine bed, machine column to foundation, etc. Workpiece fixturing systems attached either to machine table or spindle are also considered as static interfaces, containing mostly bolted joints. In contrast to their main influences on machine dynamic (e.g., stiffness and damping) and thermal (e.g., resistance to heat conduction) performances, the influence of such interfaces on the geometric accuracy are overshadowed by that of the moving interfaces incorporated into those static components.

4.2. Quasi-static interfaces

Quasi-static interfaces consist of coupling joints allowing for separation and repeatable repositioning of machine tool components such as cutting tool or the workpiece between cutting actions. An example of this is the spindle/tool (or work) holder interface. Although there is no relative motion between the two components (spindle and tool holder), since one part of the interface is interchangeable (e.g., tools), the geometric accuracy of the interface has a direct influence on the machined part accuracy. The characteristics of the interface between the cutting tool and the machine tool were extensively described in literature [1,53,174]. In general, with respect to static and dynamic stiffness, spindle/tool interface is considered as the weakest link in the machining system. Geometric accuracy of these interfaces contributes towards the accuracy of the axial and radial position of the tool (or the workpiece) with respect to the machine spindle, thus resulting in the accuracy of the machined workpiece.

Most widely used tool/workpiece interfaces use variations of conical surface contact (e.g., 7/24 taper shank tooling) or hollow-shank and face surface contact (e.g., HSK tooling) as shown in Fig. 16. [53] provides a summary of comparison of both types of interfaces, stating that hollow shank HSK interfaces have better than 0.5 µm radial and axial positioning repeatability. Rivin et al. [175] proposed alternative modifications to 7/24 taper design to improve positioning accuracy in radial and axial directions as well as to provide higher stiffness.

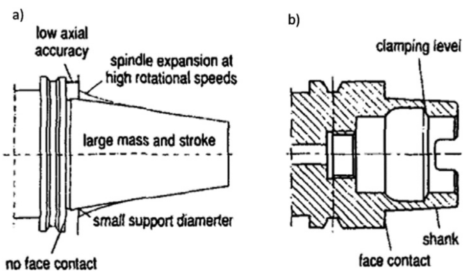

Fig. 16. Comparison of a 7/24-taper (a) and hollow shank/face contact type (b) tool holder interfaces [53].

Efforts for modeling these interfaces and their influence on accuracy of machined parts focused on stiffness and dynamic characteristics. For example, Xu et al. used FE modeling of a spindle/tool holder taper interface to predict stiffness and resulting axial and radial deformations under different clamping and spindle speed conditions [176]. Their model predicted such deformations within about 20% of the measured values. One of their conclusions was that the sliding contact at the conical interface was the main source for the axial deformation under a clamping force. In the case of workpiece fixturing systems, static stiffness is also a source of inaccuracy in machined workpieces. An example of modeling effort to predict workpiece deformation in a fixturing system is given in [177].

Various machine tool standards define the dimensions and tolerances of cylindrical and conical interfaces for attaching tool-holding and work-holding components (e.g., [178]). There are also machine tool standards to check the geometry of these interface surfaces, primarily radial, axial, and face runouts. Depending on the accessibility of the interface surfaces, these measurements either directly measure the surfaces or indirectly measure using reference artifacts mated to the interface surfaces [179]. Schematics of runout measurements, measured by displacement sensors located against the interface surfaces while those surfaces are rotated slowly, for both cases are shown in Fig. 17. The specifications of reference mandrels used for this purpose are given in [180].

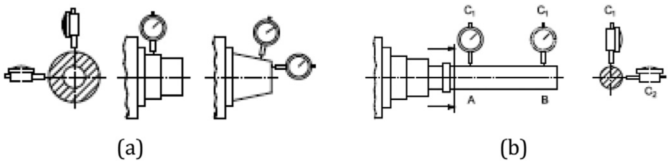

Fig. 17. Measurement of runout of (a) external interface surfaces (e.g., mounting surface for chucks on a turning center) and (b) internal taper using a mating reference mandrel [179].

Indexing rotary tables on machining centers or rotating tool turrets on turning centers are other examples for quasi-static interfaces. These interfaces enable discrete positioning of various machine tool components ensuring accurate alignment and positioning repeatability.

Machine tools requiring highest precision, such as diamond turning machines, utilize kinematic couplings for such interfaces. Kinematic couplings have the same number of contact points as the number of DOF to be constrained, therefore they are considered as deterministic systems. Achieving simple point contacts between spheres and flat surfaces as well as avoidance of bending stresses due to statically determinant structures result in high positioning repeatability [181−183]. A conventional design for such interface has three spheres on one side and geometric features on the opposite side providing six contact points as shown in Fig. 18 [181,184].

Slocum [185] developed a three-groove type kinematic coupling for fixturing large parts (250 mm diameter) on a diamond turning machine, providing closed-form analysis for the design, demonstrating 0.5 µm positioning repeatability with 45 kN cyclic preload. The kinematic coupling concept was even applied to moving interfaces in developing a micro positioning system to exploit its position repeatability while providing precise two DOF motion [186]. In this application of three-vee

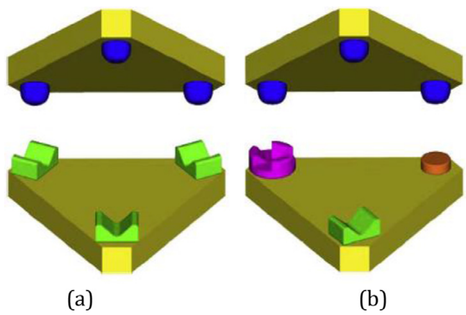

Fig. 18. Two versions of conventional design of kinematic coupling, (a) with three-groove and (b) tetrahedron-groove-flat combination (Kelvin clamp) both providing six constraints (contact points) [181].

Please cite this article as: E. Budak et al., Mechanical interfaces in machine tools, CIRP Annals - Manufacturing Technology (2022), https://doi.org/10.1016/j.cirp.2022.05.005

design, one of the balls was fixed to the moving carriage and the other two balls were moved by actuators to generate the motion of the carriage. In another variation, an adjustable kinematic coupling was designed by Rothenhöfer et al. [187] allowing for repeatable opening and closing of the interface with nanometer level height and tilt adjustability to enable tool wear compensation during machining. Semiconductor industry currently uses a standard for kinematic couplings used to align and support 300 mm wafer carriers [188].

Due to small-area (point) contacts between the balls and the mating flat surfaces resulting in high contact stresses, kinematic couplings degrade by fretting under high repetitive loading conditions. To overcome this limitation, some modifications such as arc contacts, replacing point contacts, are proposed resulting in quasi-kinematic designs with similar repeatability characteristics [189]. An extensive overview of kinematic couplings with their use in various machine tools and instruments is provided in [181].

For achieving high positioning repeatability, an alternative to the deterministic (kinematic) principle is the elastic averaging principle where the coupling is overly constrained with a large number of relatively compliant contact elements, averaging the positioning errors over the number of contact points [190]. The Hirth coupling (see Fig. 19) is a commonly used quasi-static interface in machine tools implementing the elastic averaging principle [191]. Consisting of multiple mating teeth, in addition to providing high positioning accuracy and repeatability, Hirth couplings have high torque transmission capacity and a self-centering capability while having high wear resistance due to large contact surface areas of the teeth. In a typical application of rotary indexing table of a machine tool, during machining, the mating teeth are engaged. After the end of one machining task, the teeth are disengaged, the table is rotated to its next orientation and the teeth are reengaged and constrained again for the next machining task to start. Repeatability, accuracy, and self-centering capability are necessary to produce parts within required tolerances.

An accuracy model of a rotary indexing table using Hirth coupling is given in [192]. The authors focused on the pitch error of the teeth as the main source of positioning accuracy of the table and developed a statistical model to estimate the probability density function of pitch values of the teeth and maximal pitch error. The estimated values were correlated to the measured positioning accuracy. It was shown that the positioning accuracy was improved by increasing the number of teeth.

Fig. 19. Example of Hirth coupling [191].

An analytical model of the Hirth coupling design for an indexing table, estimating irregular pressure distribution due to varying loads on the tooth flanks in the presence of friction between the mating teeth was developed in [191]. An indexing accuracy of ± 2 arcsec and repeatability of less than 1 µm were achieved. Typical geometrical testing of the resulting Hirth coupling is shown in Table 2.

Measurement of positioning accuracy of quasi-static couplings in five DOF (linear displacement along three orthogonal directions and tilt around two orthogonal axes) can be done with one setup using five displacement sensors located along three orthogonal directions detecting changes in relative position and orientation between the two components of the coupling [193]. Angular positioning error around the third axis is measured using either a precision polygon (reference angle artifact) with an autocollimator or a reference indexing table with laser interferometer/autocollimator [179]. Since the relative position and orientation between the cutting tool and the workpiece are of importance in any machining operation, the error components of the quasi-static interfaces are measured to reveal the resulting error between cutting tool and the workpiece. Fig. 20 shows a typical setup for measuring angular positioning error of an indexing table.

Table 2
Typical geometric test results of Hirth coupling [191]

Control		Theoretical measures	Tolerance	Results
Φ ext.	C1 C2 C3	990 mm	-0.01 to -0.03 mm	989.971 mm
Φ ext. Circularity	C1 C2 C3			0.005 mm
Φ int.	C1 C2 C3	849 mm H7 829 mm	+0.090 mm +0.030 mm	849.018 mm
Φ int. Circularity	C1 C2 C3			0.004 mm 0.004 mm
Concentricity Φ int. - Φ ext.	C1 C2 C3	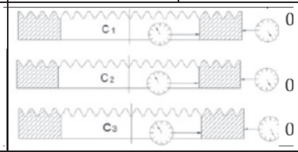		0.003 mm 0.004 mm 0.003 mm
Flatness	C1 C2 C3			0.003 mm 0.002 mm 0.002 mm
Parallelism C1-C2 Rotating C2	0° 90° 180° 270°	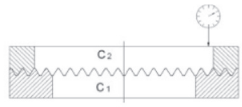		0.007 mm 0.009 mm 0.008 mm 0.009 mm
Parallelism C1-C3 Rotating C3	0° 90° 180° 270°	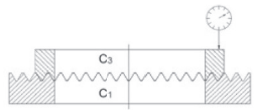		0.008 mm 0.009 mm 0.006 mm 0.009 mm
Concentricity C1-C2 Rotating C2	0° 90° 180° 270°	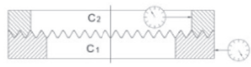		0.008 mm 0.009 mm 0.006 mm 0.009 mm
Concentricity C1-C3 Rotating C3	0° 90° 180° 270°	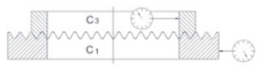		0.007 mm 0.009 mm 0.008 mm 0.009 mm
Indexing accuracy				1.5″
Hardness		HRC 54	± 2 (HRC)	HRC 54

In case of tool holding turrets on turning centers involving quasi-static interfaces (commonly Hirth couplings), both repeatability and accuracy tests of indexing are prescribed in relevant machine tool standards (e.g., [194]). Repeatability of turret indexing is measured in two orthogonal machine reference planes using a test mandrel mounted on one of the tool stations and two displacement sensors measuring the target surface along two machine axes as shown in Fig. 21. After the sensor readings are set to zero the first time, the turret is indexed 360° repeatedly to the same position and sensor readings are recorded. Maximum difference among the set of sensor readings is taken as the repeatability.

The accuracy of indexing is defined in the same standard as the maximum difference in the positions (along two axes of the machine) of the tool stations with respect to the workpiece side of the machine (work holding spindle) as the turret is indexed from one station to another in sequence. The arrangement of the displacement sensors to measure the indexing accuracy is shown in Fig. 22.

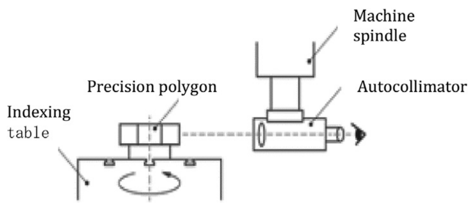

Fig. 20. Angular positioning measurement using autocollimator and polygon [179].

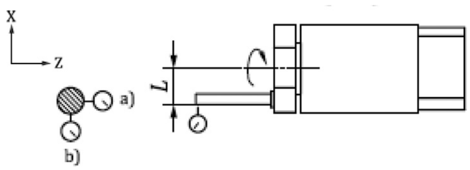

Fig. 21. A typical setup for measuring indexing repeatability of a tool holding turret in (a) YZ-plane, (b) ZX-plane of a turning center. *L* is the radial distance from the center of turret to the contact point for the displacement sensor [194].

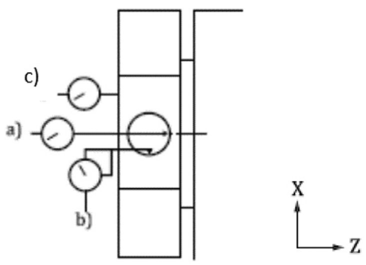

Fig. 22. A typical setup for measuring indexing accuracy of a tool holding turret (a) along Z-axis, (b) along X-axis, and (c) at the turret reference surface [194].

4.3. Moving interfaces

Moving interfaces enable linear and rotary motion of machine tool components generating mechanical work for the cutting process as well as the cutting tool path to achieve desired geometry of the machined workpiece. As such, they are among the most critical features contributing towards the geometric accuracy of a machine tool. Since they are the interfaces between at least two moving components, friction and resulting heat generation are the main concerns for the accurate performance of machine tools. Therefore, ways to reduce friction have been among the enduring efforts in precision machine tool design. From this perspective, we first classify the moving interfaces as contact and non-contact types. We then consider different alternatives in each category.

4.3.1. Contact type moving interfaces

Sliding contact (plain) interfaces

Sliding contact interfaces have good stiffness and damping characteristics which are very desirable for machine tool applications. However, stiction (static friction), high sliding friction, and resulting thermal effects and wear associated with these interfaces limit their use in machine tools. Large differences in static- and sliding-friction lead to stick-slip phenomenon, which is observed as a sudden jump in the velocity due to force level to overcome static friction being too high for overcoming the sliding friction. Many studies in the literature describe the modeling and estimation of tribological, thermal, and mechanical characteristics of sliding contact interfaces [195,196].

To improve tribological behavior of machine tool guideways with sliding interfaces, the mating surfaces are scraped to generate appropriate surface topography for hydrodynamic lubrication [197]. Some designers have used hemi-spherical pads against the flat surfaces to reduce the contact area for friction reduction purposes [198]. Plastic-based coatings are used in machine tool sliding guideways as another alternative way to reduce friction. These coatings provide self-lubricating surfaces with minimum stiction as well as heat, wear, and chemical resistance. In another study, [199] developed a friction force model introducing oscillations at the interface to reduce friction as shown in Eq. (12).

$$F_R = -\mu F_N \left[\frac{2}{\pi}\ \arcsin\left(\frac{v_f}{v_s}\right)\right] \tag{12}$$

where, $F_R$is the friction force, $F_N$is the normal force, μ is the friction coefficient, v_f is the feed velocity and v_s is the oscillating velocity. The term within the square brackets in the above equation is considered as the *friction reduction factor*. Based on this model, the authors developed a sliding bearing with ultrasonic oscillations resulting in adjustable friction characteristics avoiding stiction. The components of such adjustable friction bearing are shown in Fig. 23. The resulting reduction in positioning error is shown in Fig. 24.

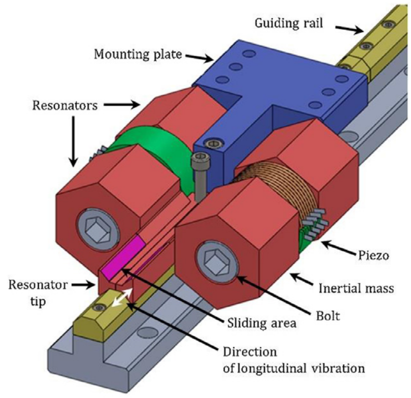

Fig. 23. Components of the adjustable friction bearing [199].

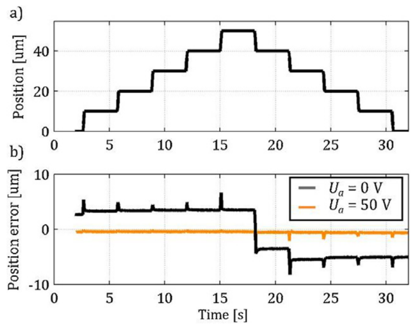

Fig. 24. Comparison of the positioning error on 10 µm steps with passive (U_a = 0 V) and active bearings (Ua = 50 V) [199].

Another effort to compensate for the stick-slip error for a high-precision table was described in [200]. A review of friction models, analysis, and compensation models can be found in [201].

Geometric accuracy of mating surfaces of sliding contact interfaces is another important source of error motions in machine tools. Therefore, depending on the design of the moving components, straightness, flatness, cylindricity, and angle between compound surfaces (e.g., for V-shaped sliding interface) need to be measured and qualified before the assembly of the machine tool. A three-probe system was presented in [202] for simultaneously measuring the straightness and parallelism of a pair of guideways. Using a probe stage which carries three displacement sensors located against the opposing surfaces of the guideways, the authors were able to mathematically eliminate probe stage error motions from measurement data to determine guideway profile errors using the reversal technique [203]. The practical methods of measurement for functional surfaces of the sliding interfaces are summarized in [179].

Rolling element contact interfaces

Rolling element interfaces are used to reduce friction between moving elements of machine tools. They make use of rotating spheres, cylinders, or other similar axisymmetric rolling elements between two interface surfaces. They are most used in spindles, rotary heads/tables, linear rail guideways, and ball screws. The

Please cite this article as: E. Budak et al., Mechanical interfaces in machine tools, CIRP Annals - Manufacturing Technology (2022), https://doi.org/10.1016/j.cirp.2022.05.005

geometric accuracies of ball bearings and cylindrical (roller) bearings used in machine tool spindles and their effects on the spindle rotational accuracy were studied extensively in literature. Some experimental studies revealed the relationship between spindle error motion frequencies and the defect frequencies of front and rear spindle bearings. A mathematical model incorporating size variation and surface waviness of rolling elements to predict bearing vibration is described in [32]. The effect of roundness error of the raceways, number of rollers, and the radial clearance on rotational accuracy of cylindrical roller bearing was studied in [204]. Based on these bearing characteristics, a mathematical model to predict the resulting radial error motion was developed. The bearing radial clearance, which is defined as the maximum displacement between inner and outer rings in radial direction, was the focus on a study in [205]. An automated measurement setup was described to measure this property after the bearing is assembled on a shaft.

Other investigators worked on improving the bearing raceway surface roughness using abrasive flow polishing technique to improve bearing performance [206]. Another example of improving geometry of roller bearing components by applying forecasting compensatory control based on measured forces during the machining of tapered rollers to reduce their roundness errors is given in [207]. 33% improvement in roundness was achieved with this strategy.

Linear guideways utilizing recirculating rolling elements to reduce friction are among the most widely used machine tool components enabling single DOF linear motion with high accuracy and stiffness (see Fig. 25).

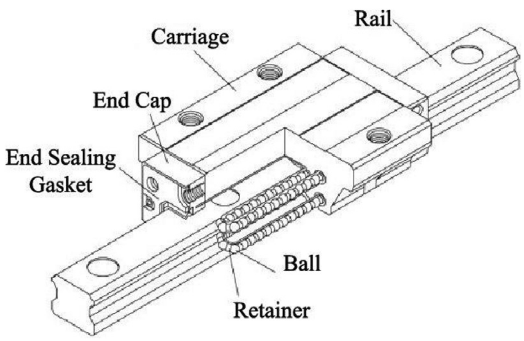

Fig. 25. Schematic of a typical linear guideway.

Authors in [208] measured and analyzed friction fluctuations due to rolling and recirculation of the balls in linear guideways affecting the motion trajectory. They studied the effects of various guideway parameters, such as preload, surface roughness of grooves and ball settings (with and without ball retainers), on the friction fluctuations. They showed that relative shift in balls between tracks could reduce friction fluctuations.

Straightness of the guideway rail directly affects the accuracy of linear motion. Zhang et al. [209] investigated the method to improve rail straightness by developing analytical and numerical models to predict the straightening stroke and longitudinal stress distribution during its manufacturing process. Similar to sliding contact interfaces, guideway rail grooves are considered as machine tool functional surfaces and their geometric errors are measured as described in [179]. A specialized instrument to measure parallelism of linear guideways, as shown in Fig. 26, is described in [210].

Another application of rolling contact interface can be found in ball screws which are used as part of the drive systems for machine tools linear positioning axes. Ball screws consist of a shaft with helical grooves (threads) and a nut with recirculating balls rolling along the shaft grooves for translating the rotational motion to linear motion with minimum friction (see Fig. 27). As such, thread profile and pitch of a ball screw are the most critical geometrical characteristics influencing the linear positioning accuracy. Conventional instruments for measuring these characteristics are coordinate measuring machines (CMM), tactile and optical profile measurement systems, and thread gauges.

Feng et al. [211] describes a measuring system utilizing a light curtain to measure ball screw thread profile. Other vision and image

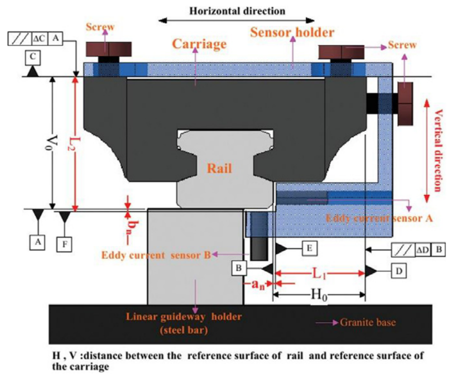

Fig. 26. Instrument for measuring parallelism of linear guideways [210].

Fig. 27. Schematic of a typical ballscrew consisting of a nut with recirculating balls and a shaft with helical grooves.

analysis based systems to measure profile and pitch of screws are described in [212–215] with a stated measurement uncertainties as low as of 0.1 μm. Another thread profile measurement system utilizing laser triangulation sensor and a dual-axis rotary stage (see Fig. 28) is described in [216].

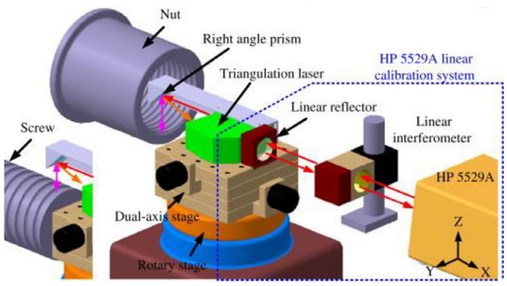

Fig. 28. Schematic of the laser-based ball screw thread profile measuring system [216].

4.3.2. Non-contact type moving interfaces

To eliminate the adverse effects of stick-slip in moving interfaces, precision machine tools utilize aerostatic, hydrostatic, hydrodynamic, or magnetic bearings for both linear guideways and rotary tables and spindles.

Aerostatic and hydrostatic interfaces

These interfaces consist of fluid bearings that use thin film of pressurized gas (aerostatic) or oil (hydrostatic) on load-bearing surfaces. The two most common types of such bearing designs utilize either porous material or small pocketed orifices to control fluid pressure and flow [217–219]. A typical orifice type aero/hydrostatic bearing is shown in Fig. 29.

Many studies investigating the accuracy of such bearings can be found in literature [220,221]. An extensive review of theory and application of hydrostatic bearings is provided in [222]. A recent

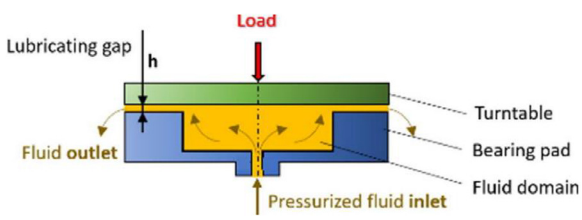

Fig. 29. Schematic of orifice type aero/hydrostatic bearing [219].

study describes the accuracy model of porous journal air bearing relating roundness errors (in terms of wave numbers) of the rotating shaft and stationary bushing of the bearing (see Fig. 30) to resulting the rotational error motion [223].

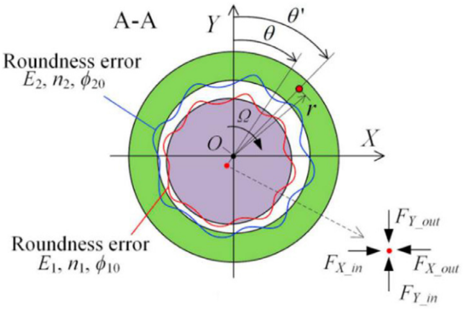

Fig. 30. Modeling the effects of roundness errors of the shaft and the bushing on rotational error motions [223].

The authors in [224] applied numerical modeling of mass flow rate to analyze stiffness, damping and the orbit of the journal center due to resulting force unbalance in the bearing. The effects of pocket shape on the performance of hydrostatic thrust pads were presented in [225]. Shimokohbe et al. developed an actively controlled (by piezo actuators) journal air bearing to improve rotational accuracy as well as stiffness and damping [226]. To improve balancing of air bearing spindles, microfluidic balancing was introduced in [227].

Due to their high-accuracy characteristics, aero/hydrostatic bearings are used mostly in high precision machine tools. Wills-Moren and Wilson [228] described a large precision grinding machine for off-axis mirror segments, which used hydrostatic guideways for horizontal linear axes and aerostatic bearings for vertical linear axis as well as the grinding spindle. High-performance slide for a small research lathe described in [229] is another example of the use of hydrostatic bearing for linear guideways. Authors in [230] developed a planar air bearing system to increase the machine tool accuracy. It is worth noting that, although hydrostatic bearings have advantage over aerostatic bearings in higher load bearing capacity and damping, they are prone to have higher thermal deformation due to high level of heat generation by the oil shear in the interfaces. Therefore, compensation for such thermal deformation plays an important role in the application of hydrostatic bearings used at high speeds [231].

Hydrodynamic interfaces

Hydrodynamic interfaces rely on relative motion between the two faces to suck fluid into the interface cavity to create an oil film wedge between the faces. These interfaces are prone to wear during starts and stops, and are therefore not widely used in machine tool applications. However, few cases were reported in literature. A spiral-type hydrodynamic bearing for machine tool spindles to achieve higher precision and stability was described in [232]. A high-precision low-speed hydrodynamic grinding spindle was described in [233] resulting in roundness and surface roughness of ground bores within 0.02 µm.

Magnetically levitated interfaces

Magnetic bearings rely on the principle of magnetic levitation to support moving parts of machine tools using a proper arrangement of electromagnets. Although they can be used in linear slides of precision instruments, they are mostly used in machine tool high-speed spindles. A simple rotating magnetic bearing is shown in Fig. 31.

The precise positioning of the rotor axis of rotation is achieved by feedback control based on displacement sensors observing the position of the rotor [234] Therefore, in addition to the geometric accuracy of the target surface (i.e., roundness of the rotor or the flatness of surface for planar bearings) the level of precision is directly affected by the quality of the sensor signal and the control algorithm used. Park et al. [235] reported a self-sensing method to eliminate the need for displacement sensors,

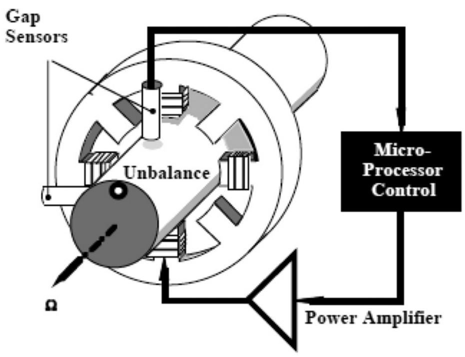

Fig. 31. Radial magnetic bearing (Ω indicates the axis of rotation) [235].

utilizing the phase difference of the injected current of two opposing actuators. A comparison of various rotor topologies of radial bearings as well as associated models and control methods was presented in [236].

Many examples of the use of magnetic bearings in machine tool applications are covered in [237–240] described an extensive study on modeling and control of machine tool magnetic spindles. Magnetic bearings were used in a spindle to improve waviness in ultra-position turning in [241]. The use of linear magnetic bearings in various machine tools and instruments are described in [70,96,242,243].

4.4. Effects of interfaces on machine tool geometric accuracy

Since the relative position and orientation between machine tool components and their intended motions are facilitated by the machine tool interfaces, geometric accuracy of these interfaces have significant and direct influence on resulting machine tool geometric accuracy. Additionally, their accuracy degradation due to misalignments and deformations resulting from the assembly process can be major contributors to machine tool geometric accuracy. The constituents of machine tool geometric accuracy consist of error motions of individual moving elements (e.g., straightness, roll, pitch, and yaw) as well as their positions and orientations with respect to each other (e.g., parallelism and squareness between axes of motion). Measurement methods of such error motions are well established in industrial standards [179,244]. A review of geometric error measurements of machine tools is given in [245]. More recent examples of using telescoping ballbars and laser interferometers in measuring position and orientation errors of machine tool components are found in [246–248].

Modeling and experimental efforts to relate the accuracy of interfaces to motion errors of machine tool components exist in literature. Investigations are described in [249,250] developing methods to calculate the straightness and angular errors of a precision linear stages based on measured profile errors of their guideways. Majda developed a finite element model of a rolling element linear guideway to estimate force-displacement characteristics of the contact elements then extended the model to describe joint kinematic errors of a machine tool table [251]. Recently, Vogl et al. [252] described the relationship between ball phases in linear guideways and the resulting error motions on the linear slide. A mathematical model of the effects of linear guideways geometrical errors on the positioning repeatability of machine tool linear axes was developed in [253]. The authors carried out a force balance analysis taking into consideration of straightness errors of the two opposing guideways supporting the carriage and determined that resulting elastic deformation was not fully recovered leading to reduced positioning repeatability. They also developed a method to determine optimum geometric errors for a desired level of repeatability using genetic algorithm.

Few studies estimated the error motions of a multi-pad type hydrostatic machine tool table using a transfer function of film reaction force in a hydrostatic pad and the form error of guide rail at various spatial frequencies obtained by finite element analysis [220]. In a similar study conducted for aerostatic guideways, Ekinci et al. developed a system of equations to describe the relationship between the guideway geometric errors and the error motions of the linear axis [254].

Interfaces of rotating elements have more direct influence on axis of rotation error motions as shown in [223]. Effects of spindle bearing errors on machine accuracy for a diamond turning machine were studied in [255]. Authors in [256] analyzed thermal deformation error of an air spindle system and provide a method to estimate and compensate this error. An early effort in spindle bearing error analysis based on industrial standards is presented in [257]. A more up to date industrial standard describing the methods for measuring and analyzing axis of rotation error motions is found in [244].

Guo et al. [258] describes the effects of assembly processes in the presence of geometric errors of components and a method to determine optimal tolerance allocation for such components based on machine tool kinematic model. In order to estimate the effects of interfaces on machine tool performance, load distribution was modeled in ball screw mechanism in [259] and mechanical vibration effects were studied on the precision of direct-drive system in [260]. Tracking errors were minimized by proposing a workpiece setup optimization algorithm for a rotary table in [261].

There are also studies developing models of entire machine tools' geometric errors including the characteristics of interfaces and linkages. In one such study, the researchers incorporated the models of spindle, tilting table bearings, and ball screws to develop a holistic model of thermal and dynamic load error for a five-axis machining center [262]. Another holistic modeling effort involved incorporating finite element modeling of air bearing linear slides into an ultra-precision micro milling machine design [263]. Authors in [264] developed the concept of elastically linked systems to correlate machine tool positional and accuracy to the geometrical and form errors of the machine parts. Examples of geometric error modeling using homogeneous coordinate transformations can be found for a turning center in [265], for a five-axis machining center [266], and for a grinding machine in [267]. Authors in [268] used actively controlled compliance device to compensate deformation of the machine tool. Positioning error due to deformation was analyzed and compensated using integrated fixturing in [269].

5. Defects and failures in contacts

Failures and defects in contacts could result in equipment failure, lost productivity and revenue, and even human casualties. As a result, detection of a problem and its location in contacts are critical for the safe and reliable operation of machinery.

5.1. Interface wear and failure

Many machine tool interfaces experience repeated rolling, sliding, stick-slip, and skidding motions under high loading conditions that cause wear and fatigue. Wear mechanisms are hard to predict as wear modes such as mating materials, working load, relative movements, speed, temperature, and lubrication conditions need to be distinguished. Bearing wear is commonly observed in machine tools, for which an international standard was developed [270]. This standard determines how failure modes are classified for bearing manufacturers. Machine tool interfaces are exposed to fatigue wear, contact fatigue, and fretting fatigue, which are significantly different from structural fatigue. Unlike structural fatigue, these fatigue types do not include endurance limits and are inevitable for contacting interfaces.

Wear fatigue term comes from the wear caused by deformations due to the asperities and surface layers when opposing surfaces contact [271]. Asperity contacts developed by very high local stresses repeated many times while sliding or rolling, and wear particles are generated by fatigue propagated cracks. The application of lubrication alleviates the level of wear during motion. However, fatigue wear is inevitable for all sliding and rolling contacts.

Contact or surface fatigue or rolling contact fatigue (RCF) terms describe the surface damage (see Fig. 32) provoked by repeated rolling contact [272]. It refers to the initial damage on a smooth surface, which shows the difference compared to fatigue wear [273], is mainly used for rolling bearings. Several mathematical models have been proposed throughout the years to predict lifetime of bearing components under

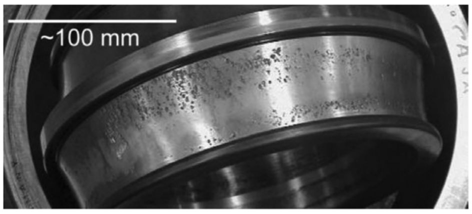

Fig. 32. RCF of inner raceway of spherical roller bearing [272].

rolling contact. Statistical and deterministic methods are two techniques employed for the prediction of bearing life.

One of the most-known equations for bearing life is introduced by Lundberg and Palmgren [273] based on statistical methods which uses Weibull distribution:

$$L_{10} = \left(\frac{C}{P}\right)^{P} \tag{13}$$

where L_{10} is the life of a bearing with a 10% chance of failure, C is the bearing's basic dynamic load rating, P is the equivalent load on the bearing, and the exponent p is 3 for ball bearings and 10/3 for roller bearings. This formula establishes the industry's first bearing life standards, and it has been widely employed since the 1950s. Although this model is a useful life prediction tool, it does not explicitly account for material microstructure. On the other hand, the deterministic models estimate the contact fatigue life based on a homogeneous description of the material in the contact zone. However, the material microstructure, which is inherently inhomogeneous due to defects and nonuniform distribution of material properties, has a significant impact on subsurface-initiated spalling. This type of spalling is the classic mode of failure in rolling elements that operate under EHL conditions [274]

Fretting fatigue is an inevitable yet unsolved factor for machine tools at low stress levels and is caused by micro-slip motion associated friction. Even solutions of frictional stationary Hertz contact problems must add micro-slip to represent a complete solution (Cattaneo–Mindlin form). The initiating mechanism for fretting fatigue is short-amplitude reciprocating sliding (micro-slip) between contacting surfaces with many cycles [271]. Some of the contacts are assumed to have no relative movement, such as interference fits, which allow micro-slip on the scale of 1 µm when alternating and oscillating loads are carried. It is very difficult to prevent or eliminate such movements, and fretting fatigue is present in almost all mechanical interfaces of machine tools.

Gross-sliding of rolling-elements on raceways causes skidding [275]. Skidding gives rise to significantly high surface shear stresses on the contact surface and is observed in bearings. Hirono's rule is extensively employed while detecting bearing gross-sliding and given in Eq. (14).

$$\frac{Q_a}{F_c} < 10 \tag{14}$$

where Q_a is the axial component of normal force and F_c is the centrifugal force [276]. Raceway control, proposed by Harris et. al., and is generally valid for high-speed bearings when the traction coefficient at the ball raceway contacts is high enough to prevent gyroscopic slip [13]. According to the analysis of Liao and Lin, increasing the deformation applied in the axial direction is an effective way to prevent the bearings from skidding at high angular velocities [277]. Tong et al. proposed a new analytical model to predict stiffness matrix of ball guides, which involves skidding, considering carriage flexibility [278]. Additionally, Tong and Hong proposed another model for the effect of angular misalignment on the running torques of tapered roller bearings [279].

Since predictive models of failure and wear are challenging to develop, online monitoring approaches have been suggested as practical strategies to prevent failures.

5.2. Defect types

Bearing faults are one of the most common mechanical sources of vibration and noise in machine tool spindles, and bearing failure is one of the most frequent types of machine failure. Although bearings are in general very reliable, they can fail due to inappropriate use, overloading, or thermal seizure [280]. Bearing faults are classified into two categories in the literature as localized and extended defects [281]. Bearing damage in which the amplitude of the ball race contact force varies constantly and periodically as the bearing rotates is known as distributed or extended defects. The damage area is large and the depth is shallow in this sort of defect [282]. Localized defects are pit or spall on the inner or outer ring, or on a rolling element (see Fig. 33), and they are the most common type of bearing failure [283]. The goal of bearing condition monitoring is to detect faults as early as possible. Over the last decades, intensive research has been done towards detecting and diagnosing bearing defects. The use of vibration analysis and signal processing to diagnose and prognose rolling element bearings has aroused a lot of attention [281].

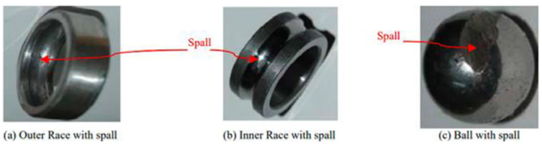

Fig. 33. Different types of spall defect on a)outer race, b)inner race and c)ball part of the bearing [284].

Ball screws are also a common failure component in machine tools due to harsh operating environment and overload. Ball screw faults include four modes of failure: lubrication starvation, preload loss, ball nut wear, and re-circulation system failure [285]. Preload loss is a major issue that has a direct impact on ball screw stiffness and rigidity, resulting in component degradation [83]. Failure of the ball screw may lead to equipment breakdown, loss of production, and even human casualties. Therefore, the fault detection and fault location of a ball screw system are important and play a curial role for the reliable operation of rotating machines.

5.3. Monitoring, diagnostics, and prognostics techniques

The early failure of the spindle bearings, as previously discussed, is one of the major issues that causes the manufacturing line to be suspended. This is usually accompanied with significant repair costs and downtime. Bearing damage can be detected and prevented as a precaution to avoid major problems.

Use of vibration signals is one of the most well-known and widely used methods for monitoring of bearing conditions. Vogl et al. [286] pointed out the root-mean-square (RMS) values of spindle housing vibrations can be compared to predetermined threshold values as one of the simplest approaches to diagnose the bearing condition [287]. High-frequency resonance [288], envelope spectrum analysis [289], wavelet transformations [290–292], neural networks [293], and synchronous sampling [294], are some of the more complex approaches.

Monitoring geometrical damages at the rolling surfaces of ball bearings is a simple and low-cost method for forecasting of bearing replacement time [295]. Sinking in and out of a cavity gives an accelerating signal like the pulsing sinus wave as shown in Fig. 34. The condition of the bearing can be analyzed using this signal.

Also, condition monitoring techniques like vibration monitoring, acoustic emission, Shock Pulse Method (SPM) and surface roughness have been successfully used for fault identification on spindle bearings [296].

As another method of diagnosing ball screw preload loss through the Hilbert-Huang Transform (HHT) and Multiscale entropy (MSE) process is proposed. The proposed method can diagnose ball screw preload loss through vibration signals when the machine tool is in operation [297]. In a different approach, Yan et al. developed a Principle Feature Analysis (PFA) wavelet field technique for selecting the most significant features from a pool of function sets to evaluate the severity of the spindle bearings defect [292].

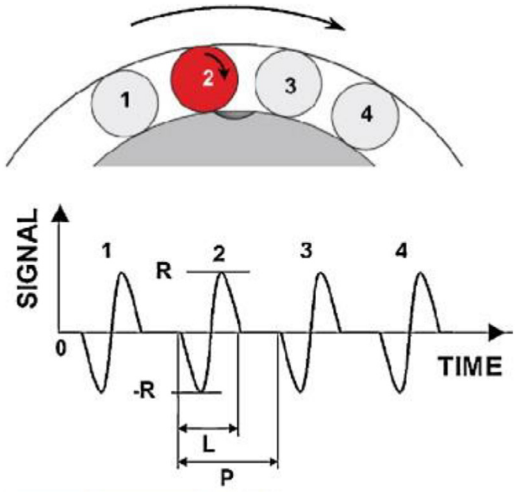

Fig. 34. Acceleration signal (R: amplitude, L: time duration, P: time period) [295].

A dynamic model is constructed by Niu et al. for investigation of high-speed rolling ball bearings with localized surface defects on raceways. By comparing the results of the simulation with tests, the model is proved to be able to effectively forecast the vibrational responses of defective high speed rolling ball bearings [298]. In other work [299], a spindle system with faulty bearings is simulated by a FE model. The vibration responses of a spindle system with various types of faulty bearings are simulated, and their vibration characteristics are analyzed and discussed in both time and frequency domains, which may give useful information for spindle status monitoring and fault diagnosis.

For a low and high-frequency signal detected under a high noise, either a high frequency of sampling or a great number of sample points are necessary for the existing large stochastic resonance (LPSR) models. A novel approach called frequency-shift and re-scaling stochastic resonance (FRSR) is developed [300], in order to overcome the above constraints and increase the usability of LPSR. The proposed method is used successfully to the diagnosis of defects of the spindle bearing outside ring.

Another method for monitoring the conditions of the bearings is using mounted strain gages in a groove ground around the bearing outer ring. The fluctuating strain field produced by the rolling motion of the spindle bearing is analyzed by an elastic model and verified with experimental data. Based on the model, a conventional sensing scheme with strain gages mounted in a groove ground around the bearing outer ring is optimized by selecting proper sensor sizes, locations, and configurations such that signal cross-over error is minimized [301].

DEmilia et al. [302], present a reliable methodology for condition monitoring of components of high-performance centerless grinding machines. This enables the detection and localization of the defects on the ball screw. The fault detection is realized using a self-implemented classification algorithm and other pattern recognition algorithms. The diagnosis is based on acceleration and acoustic emission measurement data performed on an axis test rig using various damaged ball screws at different operating parameters. As another solution for the detection of faults in ball screws, Möhring et al. [303] represented a sensory ball screw double nut system which used strain gauges or sensory thin layers to assess pre-stress as a wear indication. Sensor data is processed by integrated electronics and wirelessly transmitted. A different method to monitor the wear of a ball screw of a CNC machining center is proposed by Li et al. [304] using a Bayesian ridge regression technique for simulating the natural frequency variation of a ball screw drive system. However, because of time-varying parameters during the machining process, such as feeding speed, cutting force, and table position, condition monitoring, and health evaluation of the feed drive system in the long-term running status are challenging. To overcome this issue a novel solution is presented by Jia et al. [305] using statistical characteristics of the dynamics of the feed drive system.

In order to make monitoring systems feasible, cost-effective, and competitive, the sensorless monitoring system can be applied to monitor the health condition of contacts. In order to reach this goal, Verl et al. [306] presented a sensorless monitoring algorithm based entirely on motor current signals accessible in position-controlled drives. The program compares current characteristic parameters with those collected when the machine was fresh. In order to monitor the ball screw preload in operational mode, Nguyen et al. [307] proposed a method using the motor current signal and the screw nut axial vibration signal. This method can be utilized as an indicator of the drive system's health.

6. Discussions and conclusions

There are different challenges in each analysis approach used for modeling of contact interfaces. The first category, analytical methods, is mostly based on tribology and can be categorized based on the solution method for predicting contact characteristics of machine tools. One can claim that there are two main challenges for the analytical models. Firstly, Hertz's contact theory has been widely employed in machine tool research, but it is mostly limited to narrow, simplified, and well-defined contact problems. Obtaining the entire components of the contact stress tensor is not possible due to unsolved complex failure mechanisms that may occur on the contact surface. Secondly, the calculation of contact angles and contact deformations contains high nonlinearity and requires iterative methods (generally Newton-Raphson) where convergence could be a problem. The second category, numerical methods, is based on computational contact mechanics problem approaches. Signorini's contact problem expresses the contact interfaces. In computational contact problems, for the prediction of contact parameters, there are two main challenges. First, calculation of contact stiffness generally requires the Newton-Raphson method due to the nonlinear optimization problem. During the solution, the "no penetration" rule dictated by Hertz-Signorini-Moreau (HSM) conditions is satisfied by varying the contact stiffness during a finite solution which causes increased contact stiffness "erroneously" to avoid penetration of the contacting node pairs. Second, the reliability of solutions varies according to the chosen computational contact method. The main difficulty in the categories mentioned above is finding complete stress tensors. However, the computational burden is another major problem for all. The third category is experimental and identification methods. In this category the most-used method to identify the contact parameters at contact interfaces is the receptance coupling technique. This technique is used to identify the contact stiffness and damping parameters at spindle bearing system, spindle-holder, and tool-holder interfaces. The most challenging issue in this technique is the identification of contacts parameters and bearing dynamics under operational conditions where high spindle speed, high cutting forces, and high temperatures emerge and thus, affect the contact interface parameters. However, this technique needs an experimental frequency response measurement to identify the contact parameters at each assembly. The fourth category is hybrid methods which combine the other three methods to overcome the mentioned challenges. That is why these methods are the most studied ones in machine tool literature. One can see that contacts at the spindles are significantly influential on machine tool performance, and they are the most studied ones in the literature. .Linear guides and feed-drive contact properties are other crucial parameters for precise machine tool movements, which have also been investigated in many studies.

The heat generation models at mechanical contacts in the spindle, guideway, and ball screw are based on several conceptualizations of the friction mechanism. The PH model employs roll, slide, and spin associated with the motion conditions of rolling elements. Although it is straightforward, the model coefficients are not always accurate for every application. The EHL model is precise in the sense that it refers to the lubrication mechanism. The calculation requires tribology parameters, and it is difficult to confirm the result in a real machine. The model validation suffers from the difficulty of directly measuring generated heat, which is diffused in heat conduction, heat transfer, and radiation. The friction measurement is helpful to check the calculation and is widely used in research.

Regarding thermal contact conductance (TCC), the models for conformal and non-conformal contacts were presented. Compared to the Hertz contact, which is typical of the conformal contacts, the non-conformal contact has complex features. The calculation with the CMY model requires the material property, surface integrity, and contact pressure at the contact surface. The difficulty again arises in model validation. One problem also lies in the difficulty of evaluating TCC in a real machine. The other problem is that the heat transfer coefficient (HTC) influences the thermal behavior of the machine. In many studies, a holistic machine model is constructed with TCCs and HTCs to calculate temperature distribution. Considering boundary condition change associated with motion in ball screws and guideways is also essential for the calculation. The uncertainty of the parameters is verified by comparing the calculation result with the measurement results. Computing techniques with thermal network and model order reduction are now being studied to downsize the model degree.

Due to their static nature, any misalignment between the mating surfaces of static interfaces can easily be corrected, therefore, their effects on the overall geometric accuracy of the machine tools have not been studied rigorously. On the other hand, quasi-static interfaces are made up of coupling joints allowing separation and repeatable repositioning of machine tool components. Among quasi-static interfaces, tool holder/spindle interface is one of the most critical interface since it has a direct influence on the machined part accuracy. Kinematic and Hirth couplings, on the other hand, are two mechanisms used in machine tool components for higher position accuracy and repeatability. Moving interfaces (linear and rotary) represent a relatively mature technology. Various modeling and measurement methods are available to characterize and improve their geometric accuracy. In a broad category they can be divided into contact and non-contact moving interfaces. Sliding and rolling contact interfaces are examples of contact moving interfaces where the main concern regarding the geometric accuracy is the friction and the resulting heat generation. In precision machine tools non-contact moving interface mechanisms are more common, including aerostatic, hydrostatic, hydrodynamic, as well as magnetic bearings for linear guideways, rotary tables, and spindles. Geometric accuracy of machine tool interfaces has a direct influence on overall geometric accuracy of the machine tools. Measurement methods of error motion of moving interfaces have been standardized and different modeling and experimental works have been developed to relate the accuracy of these interfaces to the motion error of machine tools.

Contact wear and failure mechanisms are hard to predict, which is the biggest challenge for machine tools. Interface failure mechanisms are invertible and have no endurance limit. Friction is an essential catalyzer for tangential stresses and micro-slip, even for very low stresses at static interfaces. Therefore, bearing fault detection has significant importance, especially for spindles, and categorizing them helps monitor techniques. The wear failure detection is mostly focused on bearing rolling elements and ball-screw drive system.

7. Future outlook

Advancements on different contact mechanics perspectives of tribology and continuum mechanics shape the future of the machine tool interfaces. The impact of these advancements on machine tool research will rely on the adaptability of the advancements to digitalization, which requires fast and accurate prediction of interface properties. From this point of view, future research should be dedicated to fast and reliable distinction and rapid assessment of evolving boundary conditions with the possible simplest contact models. Another need is to avoid convergence problems together with quick evolution techniques for the nonlinear solution algorithms. In addition to analytical and numerical modeling approaches, the interface parameter identification techniques also need to be improved. While most of the contact parameters are based on idle state and constant temperature conditions, accurate and applicable methods for varying boundary conditions still need to be enhanced. By means of the digital twin, active connecting systems can be developed to tune the contact dynamics of tooling and clamping systems for robust and constant tool and workpiece FRF during varying loads under operational conditions. Especially on rotating components such as spindle bearings, spindle-holder, and holder-tool interfaces where sensor implementation is not feasible, accurate contact models are needed to tackle the effect of the varying loads and thermal issue on interface contact identification. Furthermore, coupling smart machine interfaces with novel and unconventional sensor systems is required for digital twin system updates of machine tools. This smart communicative mechanical interface can make feasible the concept of “smart bearings” for spindle bearings.

Modeling of heat generation and thermal transfer at the mechanical interface has been studied for a long time. Classical research focused on physical features, and the outcomes have been succeeded by the research aiming at the design and optimization of the machine system. High demand from the industry for digital twins motivates its application for the modeling of actual machines. However, the mechanical and chemical conditions linked to surrounding elements and the environment affect the heat generation and diffusion at the mechanical interface. The modeling and validation techniques that integrate elements with unknown interfaces are now being focused on and will be studied continuously, where classical models will be revisited and extended. Regarding thermal modeling of interfaces, thermal properties of the components at different working conditions and ambient temperature should be modeled to enhance prediction accuracy. Models need to be improved by considering all sources of heat transfer through mechanical interfaces where their effects are not negligible. Considering technological and digitalization developments, models need to be developed to couple and work with real data obtained by various new sensors and devices. In this regard, due to their rapid computational time, analytical models have the potential to be linked with monitoring systems. The development of thermal interfaces from design and control viewpoints, which was not introduced in this keynote, is another field for future research.

Regarding modeling of dynamic aspects of mechanical interface affecting their precision and accuracy, further improvement is required to model the damping properties of the structure since experimental identification cannot be an effective method in future versatile machine tools.

Rolling element bearings suffer from thermal expansion at high speeds due to heat generated by the friction. Such thermal expansion results in preload variations or joint deformations in overly constrained systems, which are not uncommon in machine tools for increased stiffness. There have been design efforts to maintain constant preload by floating one end of the bearing and exerting varying external hydraulic or pneumatic pressure. Such self-compensating designs are needed for various types of rolling element bearings, including the ones used in high-speed linear motion. Furthermore, since such interfaces are highly susceptible to wear, new wear resistant materials/coatings for the contact surfaces are needed to reduce operating costs.

Although demand for more precision leads to more widespread application of non-contact interfaces, their negative effects on dynamic performance (low joint damping and pneumatic hammer instability in aerostatic bearings) require special attention. In non-contact hydrostatic air or oil bearings, the air/oil gap significantly influences dynamic stiffness. Smaller gaps result in higher stiffness and higher eigenfrequencies, but lower load carrying capacity. Furthermore, shear heating and evaporative cooling of the mating surfaces of such interfaces affect the overall thermal balance of the machine tool structure. Better design optimization tools to take into account and to alleviate these effects are needed. Recent attempts to model bearing characteristics, employing CFD tools for 3D gas flow models, resistance network method for squeeze film effects, and multi-rigid-body dynamic modeling tools, are promising More sophisticated modeling for these interfaces combining their geometric, thermal, and dynamic characteristics need special attention in the future.

Advancements in the fusion of sensing and modeling of geometric accuracy of interfaces as well as new and efficient data analytics tools provide significant opportunities in improving the accuracy and precision of machine tool interfaces. Future machine tools will increasingly utilize integrated monitoring systems. As a result, precision and accuracy of mechanical interfaces will improve by embedding advanced miniaturized sensors and actuators (e.g., magnetic actuators) to detect and compensate for motion errors in moving components. With the miniaturization of linear and angular displacement sensors, it is now possible to integrate many of the off-line measurement methods and instruments into the machine tool components providing real-time information about motion accuracies of various linear and rotary machine axes. Such capabilities will enable better control/error compensation techniques and algorithms. Furthermore, incorporating various types of sensors to the machine tool interfaces and applying advanced data analytics, such as pattern recognition, machine learning, and artificial intelligence, will enable early and robust detection, diagnostics, and prognostic of the conditions of these interfaces eliminating unexpected disruptions to production schedules, thus improving productivity. However, such sensor fusion and machine learning tools have to be computationally efficient and fast to detect performance degradations in real time and should have low false negative rates to avoid unnecessary disruptions to manufacturing operations, which counteract any potential productivity gains.

Combination of advanced interface modeling capabilities with embedded sensing should enable more realistic digital twins of machine tools reflecting the machine’s real-time performance status for task optimization and effective plant level manufacturing asset management.

Interface wear and failure are inevitable for contacts. Prediction and distinguishment of wear modes are the most critical missing link in the literature. Since these mechanisms are inevitable, health monitoring systems are a must for enhancement of digitalization and virtual machine tool concepts. Therefore, the easy-to-implement and reliable monitoring systems will drive the future of machine tool research. In this regard, the contact interfaces can be monitored in a real-time manner by employing sensors to identify and detect tribological and thermal failures under operational conditions.

Declaration of Competing Interest

The authors declare that they have no known competing financial interests or personal relationships that could have appeared to influence the work reported in this paper.

Acknowledgments

The authors would like to thank all CIRP colleagues and experts who provided input for this keynote paper. Many thanks are extended to Esra Yuksel. This paper would not have been realized without her dedicated effort. Special thanks to K. Rahimzadeh, H. Jamshidi., F. Tehranizadeh who have provided important support. The authors also thank Dr. A. Archenti for valuable feedback.

Certain commercial entities or products may be identified in this document, e.g., to describe concepts adequately. Such identification is not intended to imply recommendation or endorsement by the authors or their organizations, nor to imply that the entities or products are necessarily the best available for the purpose.

References

[1] Agapiou J, Rivin E, Xie C (1995) Toolholder/spindle interfaces for CNC machine tools. *CIRP Ann.* 44(1):383–387.
[2] Popov VL, Heß M, Willert E (2019) *Handbook of Contact Mechanics : Exact Solutions of Axisymmetric Contact Problems*, Springer Nature PP - BerlinHeidelberg.
[3] Galin LA (2008) *Contact problems: the legacy of LA Galin*, 155, Springer Science & Business Media.
[4] Yan W, Komvopoulos K (1998) Contact analysis of elastic-plastic fractal surfaces. *J. Appl. Phys.* 84(7):3617–3624.
[5] Palmgren A (1959) Ball and roller bearing engineering. *Philadelphia SKF Ind. Inc* .
[6] Houpert L (Oct. 1997) A uniform analytical approach for ball and roller bearings calculations. *J. Tribol.* 119(4):851–858.
[7] Hernot X, Sartor M, Guillot J (2000) Calculation of the stiffness matrix of angular contact ball bearings by using the analytical approach. *J. Mech. Des.* 122(1):83–90.
[8] Pruvot FC, Mottu A (1980) High speed bearings for machine tool spindles. *CIRP Ann* 29(1):293–297.
[9] Jedrzejewski J, Kwasny W (2010) Modelling of angular contact ball bearings and axial displacements for high-speed spindles. *CIRP Ann* 59(1):377–382.
[10] Wock M, Spachtholz G (2003) 3-and 4-contact point spindle bearings—a new approach for high speed spindle systems. *CIRP Ann* 52(1):311–316.

[11] Yuksel E, Budak E, Ozlu E, Oral A, Igrek F, Tosun F (2021) Prediction of thermal growth in a high-speed spindle by considering thermo-mechanical behavior. *MM Sci. J.* 2021(July):4526–4533.
[12] Jones AB (Jun. 1960) A general theory for elastically constrained ball and radial roller bearings under arbitrary load and speed conditions. *J. Basic Eng.* 82(2):309–320.
[13] T. Harris, M. Kotzalas, and N. Michael, "Roller bearing analysis: advanced concepts of bearing technology." New York: Francis & Taylor, 2007.
[14] de Mul JM, Vree JM, Maas DA (Jan. 1989) Equilibrium and associated load distribution in ball and roller bearings loaded in five degrees of freedom while neglecting friction—part ii: application to roller bearings and experimental verification. *J. Tribol.* 111(1):149–155.
[15] Antoine J-F, Abba G, Molinari A (Jun. 2005) A new proposal for explicit angle calculation in angular contact ball bearing. *J. Mech. Des.* 128(2):468–478.
[16] Liao NT, Lin JF (2001) A new method for the analysis of deformation and load in a ball bearing with variable contact angle. *J. Mech. Des.* 123(2):304–312.
[17] Liu J, Ma C, Wang S, Wang S, Yang B (2019) Contact stiffness of spindle-tool holder based on fractal theory and multi-scale contact mechanics model. *Mech. Syst. Signal Process.* 119:363–379.
[18] Min X, Shuyun J, Ying C (2007) An improved thermal model for machine tool bearings. *Int. J. Mach. Tools Manuf.* 47(1):53–62.
[19] Jiang S, Zheng Y, Zhu H (Nov. 2009) A contact stiffness model of machined plane joint based on fractal theory. *J. Tribol.* 132(1).
[20] Zhao Y, Wu H, Liu Z, Cheng Q, Yang C (2018) A novel nonlinear contact stiffness model of concrete−steel joint based on the fractal contact theory. *Nonlinear Dyn* 94(1):151–164.
[21] Gupta PK (1979) Dynamics of rolling-element bearings—Part I: cylindrical roller bearing analysis. *ASME. J. Lubr. Tech* 101(3):293–302.
[22] Gupta PK (1979) Dynamics of rolling-element bearings—Part II: cylindrical roller bearing results. *ASME. J. Lubr. Tech* 101(3):305–311.
[23] Gupta PK (1979) Dynamics of rolling-element bearings—Part III: Ball bearing analysis. *ASME. J. Lubr. Tech* 101(3):312–318.
[24] Gupta PK (1979) Dynamics of rolling-element bearings—part IV: Ball bearing results. *ASME. J. Lubr. Tech* 101(3):319–326.
[25] Niu L, Cao H, He Z, Li Y (2014) Dynamic modeling and vibration response simulation for high speed rolling ball bearings with localized surface defects in raceways. *J. Manuf. Sci. Eng.* 136(4).
[26] Niu L, Cao H, He Z, Li Y (2016) An investigation on the occurrence of stable cage whirl motions in ball bearings based on dynamic simulations. *Tribol. Int.* 103:12–24.
[27] Cao H, Li Y, Chen X (2016) A new dynamic model of ball-bearing rotor systems based on rigid body element. *J. Manuf. Sci. Eng.* 138(7).
[28] Jorgensen BR, Shin YC (1998) Dynamics of spindle-bearing systems at high speeds including cutting load effects. *ASME. J. Manuf. Sci. Eng* 120(2):387–394.
[29] Changqing B, Qingyu X (2006) Dynamic model of ball bearings with internal clearance and waviness. *J. Sound Vib.* 294(1−2):23–48.
[30] Zhang J, Zhang H, Du C, Zhao W (2016) Research on the dynamics of ball screw feed system with high acceleration. *Int. J. Mach. Tools Manuf.* 111:9–16.
[31] Tlusty J, Livingston IV R, Teng YB (1986) Nonlinearities in spindle bearings and their effects. *CIRP Ann* 35(1):269–273.
[32] Lynagh N, Rahnejat H, Ebrahimi M, Aini R (2000) Bearing induced vibration in precision high speed routing spindles. *Int. J. Mach. Tools Manuf.* 40(4):561–577.
[33] Chen JS, Hwang YW (2006) Centrifugal force induced dynamics of a motorized high-speed spindle. *Int. J. Adv. Manuf. Technol.* 30(1−2):10–19.
[34] Gao X, Li B, Hong J, Guo J (2016) Stiffness modeling of machine tools based on machining space analysis. *Int. J. Adv. Manuf. Technol.* 86(5):2093–2106.
[35] Kikuchi N, Oden JT (1988) *Contact problems in elasticity: a study of variational inequalities and finite element methods*, SIAM.
[36] Yuksel E, Erturk AS, Budak E (2020) A hybrid contact implementation framework for finite element analysis and topology optimization of machine tools. *J. Manuf. Sci. Eng.* 142.
[37] Wriggers P, Zavarise G (2004) Computational contact mechanics. *Encycl. Comput. Mech.* .
[38] Aoyama T, Inasaki I (2001) Performances of HSK tool interfaces under high rotational speed. *CIRP Ann* 50(1):281–284.
[39] Hanna IM, Agapiou JS, Stephenson DA (2002) Modeling the HSK toolholder-spindle interface. *J. Manuf. Sci. Eng.* 124(3):734–744.
[40] Law M, Altintas Y, Srikantha Phani A (2013) Rapid evaluation and optimization of machine tools with position-dependent stability. *Int. J. Mach. Tools Manuf.* 68:81–90.
[41] Yüksel E, Budak E, Ertürk AS (2017) The effect of linear guide representation for topology optimization of a five-axis milling machine. *Procedia Cirp* 58:487–492.
[42] Singh S, Köpke UG, Howard CQ, Petersen D (2014) Analyses of contact forces and vibration response for a defective rolling element bearing using an explicit dynamics finite element model. *J. Sound Vib.* 333(21):5356–5377.
[43] Dadalau A, Groh K, Reuß M, Verl A (2012) Modeling linear guide systems with CoFEM: equivalent models for rolling contact. *Prod. Eng.* 6(1):39–46.
[44] Brecher C, Fey M, Tenbrock C, Daniels M (2016) Multipoint constraints for modeling of machine tool dynamics. *J. Manuf. Sci. Eng.* 138(5).
[45] Kolar P, Sulitka M, Janota M (2011) Simulation of dynamic properties of a spindle and tool system coupled with a machine tool frame. *Int. J. Adv. Manuf. Technol.* 54(1):11–20.
[46] Law M, Phani AS, Altintas Y (2013) Position-dependent multibody dynamic modeling of machine tools based on improved reduced order models. *J. Manuf. Sci. Eng.* 135(2).
[47] Zaeh M, Siedl D (2007) A new method for simulation of machining performance by integrating finite element and multi-body simulation for machine tools. *CIRP Ann* 56(1):383–386.
[48] Deng C, Liu Y, Zhao J, Wei B, Yin G (2017) Analysis of the machine tool dynamic characteristics in manufacturing space based on the generalized dynamic response model. *Int. J. Adv. Manuf. Technol.* 92(1):1411–1424.
[49] Zeljkovic M, Gatalo R, Kalajdzic M (1999) Experimental and computer aided analysis of high-speed spindle assembly behaviour. *CIRP Ann* 48(1):325–328.
[50] Matsubara A, Yamazaki T, Ikenaga S (2013) Non-contact measurement of spindle stiffness by using magnetic loading device. *Int. J. Mach. Tools Manuf.* 71:20–25.
[51] Li J, Zhu Y, Yan K, Yan X, Liu Y, Hong J (2018) Research on the axial stiffness softening and hardening characteristics of machine tool spindle system. *Int. J. Adv. Manuf. Technol.* 99(1):951–963.
[52] Chen J-S, Chen K-W (2005) Bearing load analysis and control of a motorized high speed spindle. *Int. J. Mach. Tools Manuf.* 45(12−13):1487–1493.
[53] Weck M, Schubert I (1994) New interface machine/tool: hollow shank. *CIRP Ann* 43(1):345–348.
[54] Zatarain M, Le Maître F (1989) Behaviour of covering materials for guideways. *CIRP Ann* 38(1):389–392.
[55] Fan K-C, Chen H-M, Kuo T-H (2012) Prediction of machining accuracy degradation of machine tools. *Precis. Eng.* 36(2):288–298.
[56] Schmitz TL, Donalson RR (2000) Predicting high-speed machining dynamics by substructure analysis. *Cirp Ann* 49(1):303–308.
[57] Schmitz TL, Davies MA, Medicus K, Snyder J (2001) Improving high-speed machining material removal rates by rapid dynamic analysis. *CIRP Ann* 50(1):263–268.
[58] Schmitz TL, Davies MA, Kennedy MD (2001) Tool point frequency response prediction for high-speed machining by RCSA. *J. Manuf. Sci. Eng.* 123(4):700–707.
[59] Schmitz TL, Duncan GS (2005) Three-component receptance coupling substructure analysis for tool point dynamics prediction. *ASME. J. Manuf. Sci. Eng. vol.* 127 (4):781–790.
[60] Namazi M, Altintas Y, Abe T, Rajapakse N (2007) Modeling and identification of tool holder-spindle interface dynamics. *Int. J. Mach. Tools Manuf.* 47(9):1333–1341.
[61] Matthias W, Özşahin O, Altintas Y, Denkena B (2016) Receptance coupling based algorithm for the identification of contact parameters at holder−tool interface. *CIRP J. Manuf. Sci. Technol.* 13:37–45.
[62] Schmitz T, Honeycutt A, Gomez M, Stokes M, Betters E (2019) Multi-point coupling for tool point receptance prediction. *J. Manuf. Process.* 43:2–11.
[63] Movahhedy MR, Gerami JM (2006) Prediction of spindle dynamics in milling by sub-structure coupling. *Int. J. Mach. Tools Manuf.* 46(3−4):243–251.
[64] Schmitz TL, Powell K, Won D, Duncan GS, Sawyer WG, Ziegert JC (2007) Shrink fit tool holder connection stiffness/damping modeling for frequency response prediction in milling. *Int. J. Mach. Tools Manuf.* 47(9):1368–1380.
[65] Ahmadi K, Ahmadian H (2007) Modelling machine tool dynamics using a distributed parameter tool−holder joint interface. *Int. J. Mach. Tools Manuf.* 47 (12−13):1916–1928.
[66] Ahmadian H, Nourmohammadi M (2010) Tool point dynamics prediction by a three-component model utilizing distributed joint interfaces. *Int. J. Mach. Tools Manuf.* 50(11):998–1005.
[67] Park SS, Chae J (2008) Joint identification of modular tools using a novel receptance coupling method. *Int. J. Adv. Manuf. Technol.* 35(11−12):1251–1262.
[68] Rezaei MM, Movahhedy MR, Moradi H, Ahmadian MT (2012) Extending the inverse receptance coupling method for prediction of tool-holder joint dynamics in milling. *J. Manuf. Process.* 14(3):199–207.
[69] Özşahin O, Ertürk A, Özgüven HN, Budak E (2009) A closed-form approach for identification of dynamical contact parameters in spindle−holder−tool assemblies. *Int. J. Mach. Tools Manuf.* 49(1):25–35.
[70] Albertelli P, Goletti M, Monno M (2013) A new receptance coupling substructure analysis methodology to improve chatter free cutting conditions prediction. *Int. J. Mach. Tools Manuf.* 72:16–24.
[71] Mehrpouya M, Graham E, Park SS (2013) FRF based joint dynamics modeling and identification. *Mech. Syst. Signal Process.* 39(1−2):265–279.
[72] Ertürk A, Özgüven HN, Budak E (2006) Analytical modeling of spindle-tool dynamics on machine tools using Timoshenko beam model and receptance coupling for the prediction of tool point FRF. *Int. J. Mach. Tools Manuf.* 46(15):1901–1912.
[73] Özgüven HN (1990) Structural modifications using frequency response functions. *Mech. Syst. Signal Process.* 4(1):53–63.
[74] Budak E, Ertürk A, Özgüven HN (2006) A modeling approach for analysis and improvement of spindle-holder-tool assembly dynamics. *CIRP Ann* 55 (1):369–372.
[75] Ertürk A, Budak E, Özgüven HN (2007) Selection of design and operational parameters in spindle−holder−tool assemblies for maximum chatter stability by using a new analytical model. *Int. J. Mach. Tools Manuf.* 47(9):1401–1409.
[76] Kivanc EB, Budak E (2004) Structural modeling of end mills for form error and stability analysis. *Int. J. Mach. Tools Manuf.* 44(11):1151–1161.
[77] Özşahin O, Özgüven HN, Budak E (2014) Analytical modeling of asymmetric multi-segment rotor - Bearing systems with Timoshenko beam model including gyroscopic moments. *Comput. Struct.* 144:119–126.
[78] Özşahin O, Budak E, Özgüven HN (2015) In-process tool point FRF identification under operational conditions using inverse stability solution. *Int. J. Mach. Tools Manuf.* 89:64–73.
[79] Postel M, Özsahin O, Altintas Y (2018) High speed tooltip FRF predictions of arbitrary tool-holder combinations based on operational spindle identification. *Int. J. Mach. Tools Manuf.* 129:48–60.
[80] Özşahin O, Budak E, Özgüven HN (2015) Identification of bearing dynamics under operational conditions for chatter stability prediction in high speed machining operations. *Precis. Eng.* 42:53–65.
[81] Mori K, Kono D, Yamaji I, Matsubara A (2016) Vibration reduction of machine tool using viscoelastic damper support. *Procedia CIRP* 46:448–451.
[82] Powałka B, Okulik T (2012) Dynamics of the guideway system founded on casting compound. *Int. J. Adv. Manuf. Technol.* 59(1−4):1–7.
[83] Feng G-H, Pan Y-L (2012) Investigation of ball screw preload variation based on dynamic modeling of a preload adjustable feed-drive system and spectrum analysis of ball-nuts sensed vibration signals. *Int. J. Mach. Tools Manuf.* 52(1):85–96.
[84] Wang QY, Jiang Z, Qian WM, Qi HS, Zheng HW (1993) Research on machine tools rolling slideways assembly with damping oil-films. *CIRP Ann* 42(1):441–444.
[85] DeBra DB (1992) Vibration Isolation of Precision Machine Tools and Instruments. *CIRP Ann* 41(2):711–718.
[86] Rivin EI (1995) Vibration isolation of precision equipment. *Precis. Eng.* 17(1):41–56.
[87] Shirahama Y, Sato R, Takasuka Y, Nakatsuji H, Shirase K (2016) Machine bed support with sliding surface for improving the motion accuracy. *Int. J. Autom. Technol.* 10(3):447–454.

[88] Mori K, Kono D, Yamaji I, Matsubara A (2018) Model-based installation of viscoelastic damper support for reduction of residual vibration. *Int. J. Autom. Technol.* 12(5):650–657.
[89] Huang Z, Hinduja S (1986) Shape optimization of a foundation for a large machine tool. *Int. J. Mach. Tool Des. Res.* 26(2):85–97.
[90] Peukert BW, Archenti A (2020) Dynamic interaction between precision machine tools and their foundations. *Int. J. Autom. Technol.* 14(3):386–398.
[91] Mori K, Kono D, Yamaji I, Matsubara A (2015) Support placement for machine tools using stiffness model. *Int. J. Autom. Technol.* 9(6):680–688.
[92] Mori K, Kono D, Matsubara A (2019) A robust level error estimation method for machine tool installation. *Precis. Eng.* 58:70–76.
[93] Lee W, Lee C-Y, Jeong YH, Min B-K (2015) Friction compensation controller for load varying machine tool feed drive. *Int. J. Mach. Tools Manuf.* 96:47–54.
[94] Zhao P, Huang J, Shi Y (2017) Nonlinear dynamics of the milling head drive mechanism in five-axis CNC machine tools. *Int. J. Adv. Manuf. Technol.* 91(9):3195–3210.
[95] Padmanabhan KK (1992) Prediction of damping in machined joints. *Int. J. Mach. Tools Manuf.* 32(3):305–314.
[96] h. M. Week E, Wahner U (1998) Linear magnetic bearing and levitation system for machine tools. *CIRP Ann* 47(1):311–314.
[97] Jiang S, Mao H (2010) Investigation of variable optimum preload for a machine tool spindle. *Int. J. Mach. Tools Manuf.* 50(1):19–28.
[98] Zivkovic A, Zeljkovic M, Tabakovic S, Milojevic Z (2015) Mathematical modeling and experimental testing of high-speed spindle behavior. *Int. J. Adv. Manuf. Technol.* 77(5−8):1071–1086.
[99] Guo H, Zhang J, Feng P, Wu Z, Yu D (2015) A virtual material-based static modeling and parameter identification method for a BT40 spindle−holder taper joint. *Int. J. Adv. Manuf. Technol.* 81(1):307–314.
[100] Chlebus E, Dybala B (1999) Modelling and calculation of properties of sliding guideways. *Int. J. Mach. Tools Manuf.* 39(12):1823–1839.
[101] Zaeh MF, Oertli T, Milberg J (2004) Finite element modelling of ball screw feed drive systems. *CIRP Ann* 53(1):289–292.
[102] Okwudire CE, Altintas Y (2009) Hybrid modeling of ball screw drives with coupled axial, torsional, and lateral dynamics. *J. Mech. Des.* 131(7).
[103] Archenti A, Nicolescu M (2017) A top-down equivalent stiffness approach for prediction of deviation sources in machine tool joints. *CIRP Ann* 66(1):487–490.
[104] Bonnemains T, Chanal H, Bouzgarrou B-C, Ray P (2009) Stiffness computation and identification of parallel kinematic machine tools. *J. Manuf. Sci. Eng.* 131(4).
[105] Chang Y, et al. (2020) Effect of joint interfacial contact stiffness on structural dynamics of ultra-precision machine tool. *Int. J. Mach. Tools Manuf.* 158:103609.
[106] Choi S-T, Mau S-Y (2001) Dynamic analysis of geared rotor-bearing systems by the transfer matrix method. *J. Mech. Des.* 123(4):562–568.
[107] Jiang S, Zheng S (2010) Dynamic design of a high-speed motorized spindle-bearing system. *J. Mech. Des.* 132(3).
[108] Jiang S, Zheng S (2010) A modeling approach for analysis and improvement of spindle-drawbar-bearing assembly dynamics. *Int. J. Mach. Tools Manuf.* 50(1):131–142.
[109] Cao Y, Altintas Y (2004) A general method for the modeling of spindle-bearing systems. *J Mech. Des.* 126(6):1089–1104.
[110] Cao H, Holkup T, Altintas Y (2011) A comparative study on the dynamics of high speed spindles with respect to different preload mechanisms. *Int. J. Adv. Manuf. Technol.* 57(9−12):871–883.
[111] Brouwer MD, Sadeghi F (2017) Investigation of turbocharger dynamics using a combined explicit finite and discrete element method rotor−cartridge model. *J. Tribol.* 139(1).
[112] A. Ashtekar and F. Sadeghi, "A new approach for including cage flexibility in dynamic bearing models by using combined explicit finite and discrete element methods," 2012.
[113] Xi S, Cao H, Chen X, Niu L (2018) A dynamic modeling approach for spindle bearing system supported by both angular contact ball bearing and floating displacement bearing. *J. Manuf. Sci. Eng.* 140(2).
[114] Li H, Shin YC (2004) Integrated dynamic thermo-mechanical modeling of high speed spindles, part 1: model development. *J. Manuf. Sci. Eng.* 126(1):148–158.
[115] Li H, Shin YC (2004) Analysis of bearing configuration effects on high speed spindles using an integrated dynamic thermo-mechanical spindle model. *Int. J. Mach. Tools Manuf.* 44(4):347–364.
[116] Semm T, Nierlich MB, Zaeh MF (2019) Substructure coupling of a machine tool in arbitrary axis positions considering local linear damping models. *J. Manuf. Sci. Eng.* 141(7).
[117] Irino N, et al. (2021) Vibration analysis and cutting simulation of structural nonlinearity for machine tool. *CIRP Ann* 70(1):317–320.
[118] Lin CY, Hung JP, Lo TL (2010) Effect of preload of linear guides on dynamic characteristics of a vertical column−spindle system. *Int. J. Mach. Tools Manuf.* 50(8):741–746.
[119] Mayr J, et al. (2012) Thermal issues in machine tools. *CIRP Ann* 61(2):771–791.
[120] Abele E, Altintas Y, Brecher C (2010) Machine tool spindle units. *CIRP Ann. - Manuf. Technol.* 59(2):781–802.
[121] Harris TA (2001) *Rolling bearing analysis*, John Wiley and sons.
[122] Jorgensen BR, Shin YC (Oct. 1997) Dynamics of machine tool spindle/bearing systems under thermal growth. *J. Tribol.* 119(4):875–882.
[123] Jin C, Wu B, Hu Y (2012) Heat generation modeling of ball bearing based on internal load distribution. *Tribol. Int.* 45(1):8–15.
[124] Kauschinger B, Schroeder S (2016) Uncertainties in heat loss models of rolling bearings of machine tools. *Procedia CIRP* 46:107–110.
[125] Dowson D (1995) Elastohydrodynamic and micro-elastohydrodynamic lubrication. *Wear* 190(2):125–138.
[126] Houpert L (1987) Piezoviscous-rigid rolling and sliding traction forces, application: the rolling element-cage pocket contact. *J. Tribol.* 109(2):363–370.
[127] Houpert L (1999) Numerical and analytical calculations in ball bearings. *European Space Agency-Publications-Esa Sp* 438:283–290.
[128] Balan MRD, Stamate VC, Houpert L, Tufescu A, Dumitru Olaru N (2014) Influence of the geometry on the rolling friction torque in lubricated ball-race contacts. *Appl. Mechanics and Mater.* 658:271–276.
[129] Holkup T, Cao H, Kolář P, Altintas Y, Zelený J (2010) Thermo-mechanical model of spindles. *CIRP Ann* 59(1):365–368.
[130] Brecher C, Hassis A, Rossaint J (2014) Cage friction in high-speed spindle bearings. *Tribol. Trans.* 57(1):77–85.
[131] Zheng D, Chen W (2017) Thermal performances on angular contact ball bearing of high-speed spindle considering structural constraints under oil-air lubrication. *Tribol. Int.* 109:593–601.
[132] Bossmanns B, Tu JF (2001) A power flow model for high speed motorized spindles—heat generation characterization. *J. Manuf. Sci. Eng.* 123(3):494–505.
[133] Gupta PK (2012) *Advanced dynamics of rolling elements*, Springer Science & Business Media.
[134] Li Y, Wei W, Su D, Wu W, Zhang J, Zhao W (2020) Thermal characteristic analysis of ball screw feed drive system based on finite difference method considering the moving heat source. *Int. J. Adv. Manuf. Technol.* 106(9):4533–4545.
[135] Verl A, Frey S (2010) Correlation between feed velocity and preloading in ball screw drives. *CIRP Ann* 59(1):429–432.
[136] Xu ZZ, Liu XJ, Kim HK, Shin JH, Lyu SK (2011) Thermal error forecast and performance evaluation for an air-cooling ball screw system. *Int. J. Mach. Tools Manuf.* 51(7):605–611.
[137] Jedrzejewski J, Kowal Z, Kwasny W, Winiarski Z (2019) Ball screw unit precise modelling with dynamics of loads and moving heat sources taken into account. *J. Mach. Eng.* 19(4):27–41.
[138] Oyanguren A, Larrañaga J, Ulacia I (2018) Thermo-mechanical modelling of ball screw preload force variation in different working conditions. *Int. J. Adv. Manuf. Technol.* 97(1):723–739.
[139] Olaru D, Puiu GC, Balan LC, Puiu V (2004) A new model to estimate friction torque in a ball screw system. *Product Engineering*, Springer, 333–346.
[140] Lee S-K, Yoo J-H, Yang M-S (2003) Effect of thermal deformation on machine tool slide guide motion. *Tribol. Int.* 36(1):41–47.
[141] Cheng D-J, Park J-H, Suh J-S, Kim S-J, Park C-H (2017) Effect of frictional heat generation on the temperature distribution in roller linear motion rail surface. *J. Mech. Sci. Technol.* 31(3):1477–1487.
[142] Attia MH (1988) *PhD Thesis*, McGill University.
[143] Nakajima K (1995) Thermal contact resistance between balls and rings of a bearing under axial, radial, and combined loads. *J. Thermophys. heat Transf.* 9(1):88–95.
[144] Bossmanns B, Tu JF (1999) A thermal model for high speed motorized spindles. *Int. J. Mach. Tools Manuf.* 39(9):1345–1366.
[145] Fang B, Zhang J, Wan S, Hong J (May 2018) Determination of Optimum Preload Considering the Skidding and Thermal Characteristic of High-Speed Angular Contact Ball Bearing. *J. Mech. Des.* 140(5). MD-17−1510.
[146] Yovanovich MM (2005) Four decades of research on thermal contact, gap, and joint resistance in microelectronics. *IEEE Trans. Components Packag. Technol.* 28(2):182–206.
[147] Cooper MG, Mikic BB, Yovanovich MM (1969) Thermal contact conductance. *Int. J. Heat Mass Transf.* 12(3):279–300.
[148] Mikić BB (1974) Thermal contact conductance; theoretical considerations. *Int. J. Heat Mass Transf.* 17(2):205–214.
[149] Yovanovich MM (1981) Thermal contact correlations. *16th Thermophysics Conference*, 83–95.
[150] Song S, Yovanovich MM (1987) Explicit relative contact pressure expression-Dependence upon surface roughness parameters and Vickers microhardness coefficients. *25th AIAA Aerospace Sciences Meeting*, 153.
[151] Negus KJ, Yovanovich MM (1988) Correlation of the gap conductancg integral for conforming rough surf aces. *J. Thermophys. heat Transf.* 2(3):279–281.
[152] Jiang S, Zheng Y (2011) An analytical model of thermal contact resistance based on the Weierstrass—Mandelbrot fractal function. *Proc. Inst. Mech. Eng. Part C J. Mech. Eng. Sci.* 224(4):959–967.
[153] Jedrzejewski J (1988) Effect of the thermal contact resistance on thermal behaviour of the spindle radial bearings. *Int. J. Mach. tools Manuf.* 28(4):409–416.
[154] Kim S-M, Lee S-K (2001) Prediction of thermo-elastic behavior in a spindle−bearing system considering bearing surroundings. *Int. J. Mach. Tools Manuf.* 41(6):809–831.
[155] Uhlmann E, Hu J (2012) Thermal modelling of an HSC machining centre to predict thermal error of the feed system. *Prod. Eng.* 6(6):603–610.
[156] Su H, Lu L, Liang Y, Zhang Q, Sun Y, Liu H (2014) Finite element fractal method for thermal comprehensive analysis of machine tools. *Int. J. Adv. Manuf. Technol.* 75(9−12):1517–1526.
[157] Ma C, Mei X, Yang J, Zhao L, Shi H (2015) Thermal characteristics analysis and experimental study on the high-speed spindle system. *Int. J. Adv. Manuf. Technol.* 79(1−4):469–489.
[158] Fang B, Gu T, Ye D, Luo T (2016) An improved thermo-mechanical model for vertical machining center. *Int. J. Adv. Manuf. Technol.* 87(9):2581–2592.
[159] Attia MH, Kops L (1978) On the role of fixed joints in thermal deformation of machine tool structure. *Ann. CIRP* 27(1):305.
[160] Attia MH, Kops L (1979) Nonlinear thermoelastic behavior of structural joints—solution to a missing link for prediction of thermal deformation of machine tools. *ASME. J. Eng. Ind.* 101(3):348–354.
[161] Kops L, Abrams DM (1984) Effect of shear stiffness of fixed joints on thermal deformation of machine tools. *CIRP Ann* 33(1):233–238.
[162] Rabréau C, et al. (2018) Influence of bearing kinematics hypotheses on ball bearing heat generation. *Procedia CIRP* 77:622–625.
[163] Kim SK, Cho DW (1997) Real-time estimation of temperature distribution in a ball-screw system. *Int. J. Mach. Tools Manuf.* 37(4):451–464.
[164] Yun WS, Kim SK, Cho DW (1999) Thermal error analysis for a CNC lathe feed drive system. *Int. J. Mach. tools Manuf.* 39(7):1087–1101.
[165] Liu K, Liu H, Li T, Wang Y, Sun M, Wu Y (2018) Prediction of comprehensive thermal error of a preloaded ball screw on a gantry milling machine. *J. Manuf. Sci. Eng.* 140(2). MANU-17−1130.
[166] Jędrzejewski J, Kwaśny W, Kowal Z, Winiarski Z (2014) Development of the modelling and numerical simulation of the thermal properties of machine tools. *J. Mach. Eng.* 14(3):5–20.

[167] Burghold EM, Frekers Y, Kneer R (2015) Determination of time-dependent thermal contact conductance through IR-thermography. *Int. J. Therm. Sci.* 98:148–155.
[168] Konvicka J, et al. (2004) Simulation, experimental investigation and control of thermal behavior in modular tool systems. *Nonlinear Dyn. Prod. Syst.* : 265–285.
[169] Neugebauer R, Ihlenfeldt S, Zwingenberger C (2010) An extended procedure for convective boundary conditions on transient thermal simulations of machine tools. *Prod. Eng.* 4(6):641–646.
[170] Kauschinger B, Schroeder S (2015) Uncertain parameters in thermal machine-tool models and methods to design their metrological adjustment process. *Appl. Mechan. Mater.* 794:379–387.
[171] Ihlenfeldt S, Schroeder S, Penter L, Hellmich A, Kauschinger B (2020) Adjustment of uncertain model parameters to improve the prediction of the thermal behavior of machine tools. *CIRP Ann* 69(1):329–332.
[172] Hernández-Becerro P, Spescha D, Wegener K (2021) Model order reduction of thermo-mechanical models with parametric convective boundary conditions: focus on machine tools. *Comput. Mech.* 67(1):167–184.
[173] Hernández-Becerro P, et al. (2021) Reduced-order model of the environmental variation error of a precision five-axis machine tool. *J. Manuf. Sci. Eng.* 143(2):21005.
[174] Rivin EI, et al. (2000) Tooling structure: interface between cutting edge and machine tool. *CIRP Ann* 49(2):591–634. https://doi.org/10.1016/S0007-8506(07)63457-X.
[175] E. I. Rivin, "Advanced 7/24 taper toolholder/spindle interfaces for high-speed CNC machine tools," SAE Trans., pp. 1057–1068, 1998.
[176] Xu C, Zhang J, Feng P, Yu D, Wu Z (Jul. 2014) Characteristics of stiffness and contact stress distribution of a spindle–holder taper joint under clamping and centrifugal forces. *Int. J. Mach. Tools Manuf.* 82–83:21–28.
[177] Siebenaler SP, Melkote SN (2006) Prediction of workpiece deformation in a fixture system using the finite element method. *Int. J. Mach. Tools Manuf.* 46(1):51–58.
[178] International Organization for Standardization. *"Connecting dimensions of spindle noses and work holding chucks – Part 1: Conical connection, (1),"* ISO 702-12009 Mach. tools .
[179] International Organization for Standardization. *Test code for machine tools – Part 1: Geometric accuracy of machines operating under no-load or quasi-static conditions* .
[180] ISO/TR 230-11. *Test code for machine tools – Part 11: Measuring instruments suitable for machine tool geometry tests* .
[181] Slocum A (2010) Kinematic couplings: A review of design principles and applications. *Int. J. Mach. Tools Manuf.* 50(4):310–327.
[182] Schouten CH, Rosielle P, Schellekens PHJ (1997) Design of a kinematic coupling for precision applications. *Precis. Eng.* 20(1):46–52.
[183] Slocum AH (1992) Design of three-groove kinematic couplings. *Precis. Eng.* 14 (2):67–76.
[184] Hale LC, Slocum AH (2001) Optimal design techniques for kinematic couplings. *Precis. Eng.* 25(2):114–127.
[185] Slocum AH (1988) Kinematic couplings for precision fixturing—Part I: Formulation of design parameters. *Precis. Eng.* 10(2):85–91.
[186] Taylor JB, Tu JF (1996) Precision X-Y microstagee with maneuverable kinematic coupling mechanism. *Precis. Eng.* 18(2):85–94.
[187] Rothenhöfer G, Slocum A, Kitajima T (2013) An adjustable kinematic coupling for use in machine tools with a tight structural loop. *Precis. Eng.* 37(1):61–72.
[188] SEMI E57. *Specification for kinematic couplings used to align and support 300 mm wafer carriers, available at www.semiviews.org* .
[189] Culpepper ML (2004) Design of quasi-kinematic couplings. *Precis. Eng.* 28 (3):338–357.
[190] Rowe KG, Dickrell DJ, Sawyer WG (2015) Interrupted measurement repositioning using elastic averaging. *Tribol. Lett.* 59(1):1–3.
[191] Croccolo D, De Agostinis M, Fini S, Olmi G, Robusto F, Vincenzi N (2018) On Hirth ring couplings: design principles including the effect of friction. *Actuators* 7(4):79.
[192] Bartkowiak T, Staniek R (2013) Accuracy model of rotary indexing table. *Arch. Mech. Technol. Autom.* 33(1):3–13.
[193] Slocum AH, Donmez A (1988) Kinematic couplings for precision fixturing — Part 2: Experimental determination of repeatability and stiffness. *Precis. Eng.* 10(3):115–122.
[194] International Organization for Standardization. *Test conditions for numerically controlled turning machines and turning centres – Part 1: Geometric tests for machines with horizontal workholding spindle(s),ISO 13041-1* .
[195] Majcherczak D, Dufrenoy P, Berthier Y (May 2007) Tribological, thermal and mechanical coupling aspects of the dry sliding contact. *Tribol. Int.* 40(5):834–843.
[196] Chantrenne P, Raynaud M (1997) A microscopic thermal model for dry sliding contact. *Int. J. Heat Mass Transf.* 40(5):1083–1094.
[197] Yukeng H, Darong C, Linqing Z (1985) Effect of surface topography of scraped machine tool guideways on their tribological behaviour. *Tribol. Int.* 18(2):125–129.
[198] Monteiro AF, Smith ST, Chetwynd DG (1996) A super-precision linear slideway with angular correction in three axes. *Nanotechnology* 7(1):27.
[199] Engel T, Lechler A, Verl A (2016) Sliding bearing with adjustable friction properties. *CIRP Ann* 65(1):353–356.
[200] Mei X, Tsutsumi M, Tao T, Sun N (2004) Study on the compensation of error by stick-slip for high-precision table. *Int. J. Mach. tools Manuf.* 44(5):503–510.
[201] Armstrong-Hélouvry B, Dupont P, De Wit CC (1994) A survey of models, analysis tools and compensation methods for the control of machines with friction. *Automatica* 30(7):1083–1138.
[202] Hwang J, Park C-H, Gao W, Kim S-W (2007) A three-probe system for measuring the parallelism and straightness of a pair of rails for ultra-precision guideways. *Int. J. Mach. Tools Manuf.* 47(7–8):1053–1058.
[203] Evans CJ, Hocken RJ, Estler WT (1996) Self-calibration: reversal, redundancy, error separation, and 'absolute testing. *CIRP Ann* 45(2):617–634.
[204] Yongjian Y, Guoding C, Jishun L, Yujun X (2017) Research on rotational accuracy of cylindrical roller bearings. *Procedia CIRP* 62:380–385.
[205] Meier N, Georgiadis A (2016) Automatic assembling of bearings including clearance measurement. *Procedia CIRP* 41:242–246.
[206] Wu MY, Gao H (2016) Experimental study on large size bearing ring raceways' precision polishing with abrasive flowing machine (AFM) method. *Int. J. Adv. Manuf. Technol.* 83(9–12):1927–1935.
[207] Fung EHK, Chan JCK (2000) ARX modelling and compensation of roundness errors in taper turning. *Int. J. Adv. Manuf. Technol.* 16(6):404–412.
[208] Miura T, Matsubara A, Yamaji I, Hoshide K (2018) Measurement and analysis of friction fluctuations in linear guideways. *CIRP Ann. - Manuf. Technol.* 67(1):393–396.
[209] Zhang Y, Lu H, Ling H, Lian Y, Ma M (2018) Analytical model of a multi-step straightening process for linear guideways considering neutral axis deviation. *Symmetry (Basel)* 10(8):316.
[210] Hsieh T-H, Huang H-L, Jywe W-Y, Liu C-H (2014) Development of a machine for automatically measuring static/dynamic running parallelism in linear guideways. *Rev. Sci. Instrum.* 85(3):35115.
[211] Feng H-T, Wang Y-L, Li C-M, Tao W-J (2011) An automatic measuring method and system using a light curtain for the thread profile of a ballscrew. *Meas. Sci. Technol.* 22(8):85106.
[212] Warnecke H-J, Pavel G, Kuhn G (1981) Optical Testing of Bolt-Type Screws. *CIRP Ann* 30(1):461–466.
[213] Liu C-C, Chen W-Y (2006) Screw pitch precision measurement using simple linear regression and image analysis. *Appl. Math. Comput.* 178(2):390–404.
[214] Chen TY, Hou PH, Chiu JY (2002) Measurement of the ballscrew contact angle by using the photoelastic effect and image processing. *Opt. Lasers Eng.* 38(1–2):87–95.
[215] Hunsicker RJ, Patten J, Ledford A, Ferman C, Allen M, Ellis C (1994) Automatic vision inspection and measurement system for external screw threads. *J. Manuf. Syst.* 13(5):370–384.
[216] Huang H-L, Jywe W-Y, Liu C-H, Duan L, Wang M-S (2010) Development of a novel laser-based measuring system for the thread profile of ballscrew. *Opt. Lasers Eng.* 48(10):1012–1018.
[217] Corbett J, Almond RJ, Stephenson DJ, Kwan YBP (1998) Porous ceramic water hydrostatic bearings for improved for accuracy performance. *CIRP Ann* 47(1):467–470.
[218] Stout KJ, Sweeney F (1984) Design of aerostatic flat pad bearings using pocketed orifice restrictors. *Tribol. Int.* 17(4):191–198.
[219] Michalec M, Svoboda P, Křupka I, Hartl M (2021) A review of the design and optimization of large-scale hydrostatic bearing systems. *Eng. Sci. Technol. an Int. J.* .
[220] Shamoto E, Park C-H, Moriwaki T (2001) Analysis and improvement of motion accuracy of hydrostatic feed table. *Cirp Ann* 50(1):285–290.
[221] Kawai T, Ebihara K, Takeuchi Y (2005) Improvement of machining accuracy of 5-axis control ultraprecision machining by means of laminarization and mirror surface finishing. *CIRP Ann* 54(1):329–332.
[222] Liu Z, Wang Y, Cai L, Zhao Y, Cheng Q, Dong X (2017) A review of hydrostatic bearing system: researches and applications. *Adv. Mech. Eng.* 9(10). 1687814017730536.
[223] Zhang P (2020) A study on accuracy of porous journal air bearing. *Precis. Eng.* 66:42–51.
[224] Han D, Park S, Kim W, Kim J (1994) A study on the characteristics of externally pressurized air bearings. *Precis. Eng.* 16(3):164–173.
[225] Sharma SC, Jain SC, Bharuka DK (2002) Influence of recess shape on the performance of a capillary compensated circular thrust pad hydrostatic bearing. *Tribol. Int.* 35(6):347–356.
[226] Shimokohbe A, Horikawa O, Sato K, Sato H (1991) An active air journal bearing with ultraprecision, infinite static stiffness, high damping capability and new functions. *CIRP Ann* 40(1):563–566.
[227] Dörgeloh T, Beinhauer A, Riemer O, Brinksmeier E (2016) Microfluidic balancing concepts for ultraprecision high speed applications. *Procedia CIRP* 46:185–188.
[228] Wills-Moren WJ, Wilson T (1989) The design and manufacture of a large CNC grinding machine for off-axis mirror segments. *CIRP Ann* 38(1):529–532.
[229] Donaldson RR, Maddux AS, Shaw MC (1984) Design of a High-Performance Slide and Drive System for a Small Precision Machining Research Lathe. *CIRP Ann* 33 (1):243–248.
[230] Erkorkmaz K, Gorniak JM, Gordon DJ (2010) Precision machine tool X–Y stage utilizing a planar air bearing arrangement. *CIRP Ann* 59(1):425–428.
[231] Moriwaki T (1988) Thermal Deformation and Its On-Line Compensation of Hydrostatically Supported Precision Spindle. *CIRP Ann* 37(1):393–396.
[232] Changhou L, Xing A, Jianfeng L (1998) Analysis and research on spiral oil wedge hydrodynamic bearing for precise machine tool spindles. *Int. J. Mach. Tools Manuf.* 38(3):197–203.
[233] Yingzhong L, Peters J (1982) Study on High-Precision, Low-Speed Hydrodynamic Bearing. *CIRP Ann* 31(1):299–303.
[234] Schweitzer G (2002) Active magnetic bearings-chances and limitations. *6th Int. Conf. Rotor Dyn*, 1–14.
[235] Park YH, Han DC, Park IH, Ahn HJ, Jang DY (2008) A self-sensing technology of active magnetic bearings using a phase modulation algorithm based on a high frequency voltage injection method. *J. Mech. Sci. Technol.* 22(9):1757–1764.
[236] Zhang W, Zhu H (2017) Radial magnetic bearings: An overview. *Results Phys* 7:3756–3766.
[237] Y. Honda, S. Yokote, T. Higaki, and Y. Takeda, "Using the Halbach magnet array to develop an ultrahigh-speed spindle motor for machine tools," in IAS '97. Conference Record of the 1997 IEEE Industry Applications Conference Thirty-Second IAS Annual Meeting, vol. 1, pp. 56–60.
[238] Kimman MH, Langen HH, Schmidt RHM (2010) A miniature milling spindle with active magnetic bearings. *Mechatronics* 20(2):224–235.
[239] Tamisier V, Font S, Lacour M, Carrere F, Dumur D (2001) Attenuation of vibrations due to unbalance of an active magnetic bearings milling electro-spindle. *CIRP Ann* 50(1):255–258.
[240] Sawicki JT, Maslen EH, Bischof KR (2007) Modeling and performance evaluation of machining spindle with active magnetic bearings. *J. Mech. Sci. Technol.* 21 (6):847–850.
[241] Khanfir H, Bonis M, Revel P (2005) Improving waviness in ultra precision turning by optimizing the dynamic behavior of a spindle with magnetic bearings. *Int. J. Mach. tools Manuf.* 45(7–8):841–848.
[242] Denkena B, Dahlmann D, Krueger R (2016) Design and Optimisation of an Electromagnetic Linear Guide for Ultra-Precision High Performance Cutting. *Procedia CIRP* 46:147–150.

[243] Denkena B, Dahlmann D, Krueger R (2015) Electromagnetic Levitation Guide for Use in Ultra-Precision Milling Centres. *Procedia CIRP* 37:199–204.
[244] ISO 230-7. *Test code for machine tools — Part 7: Geometric accuracy of axes of rotation* .
[245] Schwenke H, Knapp W, Haitjema H, Weckenmann A, Schmitt R, Delbressine F (2008) Geometric error measurement and compensation of machines—An update. *CIRP Ann* 57(2):660–675.
[246] Chen J, Lin S, Zhou X, Gu T (2016) A ballbar test for measurement and identification the comprehensive error of tilt table. *Int. J. Mach. Tools Manuf.* 103:1–12.
[247] Guo Y, et al. (2018) Continuous measurements with single setup for position-dependent geometric errors of rotary axes on five-axis machine tools by a laser displacement sensor. *Int. J. Adv. Manuf. Technol.* 99(5):1589–1602.
[248] Xiang S, Yang J, Zhang Y (2014) Using a double ball bar to identify position-independent geometric errors on the rotary axes of five-axis machine tools. *Int. J. Adv. Manuf. Technol.* 70(9−12):2071–2082.
[249] Tang H, Duan J, Zhao Q (2017) A systematic approach on analyzing the relationship between straightness & angular errors and guideway surface in precise linear stage. *Int. J. Mach. Tools Manuf.* 120:12–19.
[250] He G, Sun G, Zhang H, Huang C, Zhang D (2017) Hierarchical error model to estimate motion error of linear motion bearing table. *Int. J. Adv. Manuf. Technol.* 93 (5):1915–1927.
[251] Majda P (2012) Modeling of geometric errors of linear guideway and their influence on joint kinematic error in machine tools. *Precis. Eng.* 36(3):369–378.
[252] Vogl GW, Shreve KF, Donmez MA (2021) Influence of bearing ball recirculation on error motions of linear axes. *CIRP Ann* 70(1):345–348.
[253] Sun G, He G, Zhang D, Sang Y, Zhang X, Ding B (2018) Effects of geometrical errors of guideways on the repeatability of positioning of linear axes of machine tools. *Int. J. Adv. Manuf. Technol.* 98(9):2319–2333.
[254] Ekinci TO, Mayer JRR, Cloutier GM (2009) Investigation of accuracy of aerostatic guideways. *Int. J. Mach. Tools Manuf.* 49(6):478–487.
[255] Chen D, Fan J, Zhang F (2012) An identification method for spindle rotation error of a diamond turning machine based on the wavelet transform. *Int. J. Adv. Manuf. Technol.* 63(5−8):457–464.
[256] Moriwaki T, Shamoto E (1998) Analysis of thermal deformation of an ultraprecision air spindle system. *CIRP Ann* 47(1):315–319.
[257] Martin DL, Tabenkin AN, Parsons FG (1995) Precision spindle and bearing error analysis. *Int. J. Mach. Tools Manuf.* 35(2):187–193.
[258] Guo J, Liu Z, Li B, Hong J (2015) Optimal tolerance allocation for precision machine tools in consideration of measurement and adjustment processes in assembly. *Int. J. Adv. Manuf. Technol.* 80(9):1625–1640.
[259] Lin B, Okwudire CE, Wou JS (2018) Low order static load distribution model for ball screw mechanisms including effects of lateral deformation and geometric errors. *J. Mech. Des.* 140(2).
[260] Yang X, Lu D, Zhao W (2018) Decoupling and effects of the mechanical vibration on the dynamic precision for the direct-driven machine tool. *Int. J. Adv. Manuf. Technol.* 95(9):3243–3258.
[261] Yang J, Aslan D, Altintas Y (2018) Identification of workpiece location on rotary tables to minimize tracking errors in five-axis machining. *Int. J. Mach. Tools Manuf.* 125:89–98.
[262] Jedrzejewski J, Kwasny W (2012) Holistic precision error model for 5 axis HSC machining centre with rotating rolling units in direct drives. *Procedia CIRP* 4:125–130.
[263] Huo D, Cheng K, Wardle F (2010) A holistic integrated dynamic design and modelling approach applied to the development of ultraprecision micro-milling machines. *Int. J. Mach. Tools Manuf.* 50(4):335–343.
[264] Archenti A, Nicolescu M (2013) Accuracy analysis of machine tools using Elastically Linked Systems. *CIRP Ann* 62(1):503–506.
[265] Donmez MA, Blomquist DS, Hocken RJ, Liu CR, Barash MM (1986) A general methodology for machine tool accuracy enhancement by error compensation. *Precis. Eng.* 8(4):187–196.
[266] Lamikiz A, De Lacalle LNL, Ocerin O, Díez D, Maidagan E (2008) The Denavit and Hartenberg approach applied to evaluate the consequences in the tool tip position of geometrical errors in five-axis milling centres. *Int. J. Adv. Manuf. Technol.* 37(1−2):122–139.
[267] Chen GS, Mei XS, Li HL (2013) Geometric error modeling and compensation for large-scale grinding machine tools with multi-axes. *Int. J. Adv. Manuf. Technol.* 69(9−12):2583–2592.
[268] Matsumoto K, Hatamura Y, Nakao M (2000) Actively controlled compliance device for machining error reduction. *CIRP Ann* 49(1):313–316.
[269] Sanchez HT, Estrems M, Faura F (2006) Analysis and compensation of positional and deformation errors using integrated fixturing analysis in flexible machining parts. *Int. J. Adv. Manuf. Technol.* 29(3−4):239–252.
[270] ISO 15243. *Rolling bearings — Damage and failures — Terms, characteristics and causes* .
[271] Stachowiak GW, Batchelor AW (2013) Engineering tribology. *Butterworth-heinemann* .
[272] Olver AV (2005) The mechanism of rolling contact fatigue: an update. *Proc. Inst. Mech. Eng. Part J J. Eng. Tribol.* 219(5):313–330.
[273] Sadeghi F, Jalalahmadi B, Slack TS, Raje N, Arakere NK (Sep. 2009) A Review of Rolling Contact Fatigue. *J. Tribol.* 131(4).
[274] Ahmed R (2002) Rolling contact fatigue. *ASM Handb* 11:941–956.
[275] Dadouche A, Kerrouche R (2021) Bearing Skidding Detection for High Speed and Aero Engine Applications. *Turbo Expo: Power for Land, Sea, and Air* 85024. V09AT24A014.
[276] Hirano F (Jan. 1965) Motion of a Ball in Angular-Contact Ball Bearing. *A S L E Trans* 8(4):425–434.
[277] Tung Liao N, Lin JF (2002) Ball bearing skidding under radial and axial loads. *Mech. Mach. Theory* 37(1):91–113.
[278] Tong V-C, Khim G, Hong S-W, Park C-H (2019) Construction and validation of a theoretical model of the stiffness matrix of a linear ball guide with consideration of carriage flexibility. *Mech. Mach. Theory* 140:123–143.
[279] Tong V-C, Hong S-W (2016) The effect of angular misalignment on the running torques of tapered roller bearings. *Tribol. Int.* 95:76–85.
[280] Cao H, Niu L, He Z (2012) Method for vibration response simulation and sensor placement optimization of a machine tool spindle system with a bearing defect. *Sensors* 12(7):8732–8754.
[281] De Castelbajac C, Ritou M, Laporte S, Furet B (2014) Monitoring of distributed defects on HSM spindle bearings. *Appl. Acoust.* 77:159–168.
[282] Meyer LD, Ahlgren FF, Weichbrodt B (Apr. 1980) An Analytic Model for Ball Bearing Vibrations to Predict Vibration Response to Distributed Defects. *J. Mech. Des.* 102(2):205–210.
[283] Randall RB, Antoni J (2011) Rolling element bearing diagnostics—A tutorial. *Mech. Syst. Signal Process.* 25(2):485–520.
[284] Bhavaraju KM, Kankar PK, Sharma SC, Harsha SP (2010) A comparative study on bearings faults classification by artificial neural networks and self-organizing maps using wavelets. *Int. J. Eng. Sci. Technol.* 2(5):1001–1008.
[285] Jin W, Chen Y, Lee J (2013) Methodology for ball screw component health assessment and failure analysis. *ASME 2013 International Manufacturing Science and Engineering Conference Collocated with the 41st North American Manufacturing Research Conference, MSEC 2013* 2. V002T02A031.
[286] Vogl GW, Donmez MA (2015) A defect-driven diagnostic method for machine tool spindles. *CIRP Ann* 64(1):377–380.
[287] Rastegari A, Archenti A, Mobin M (2017) Condition based maintenance of machine tools: Vibration monitoring of spindle units. *2017 Annual Reliability and Maintainability Symposium (RAMS)* : 1–6.
[288] McFadden PD, Smith JD (1984) Vibration monitoring of rolling element bearings by the high-frequency resonance technique—a review. *Tribol. Int.* 17 (1):3–10.
[289] Patel VN, Tandon N, Pandey RK (2012) Defect detection in deep groove ball bearing in presence of external vibration using envelope analysis and Duffing oscillator. *Measurement* 45(5):960–970.
[290] Kulkarni PG, Sahasrabudhe AD (2017) Investigations on mother wavelet selection for health assessment of lathe bearings. *Int. J. Adv. Manuf. Technol.* 90(9):3317–3331.
[291] Liu J (2012) Shannon wavelet spectrum analysis on truncated vibration signals for machine incipient fault detection. *Meas. Sci. Technol.* 23(5):55604.
[292] Yan R, Gao RX (2011) Wavelet domain principal feature analysis for spindle health diagnosis. *Struct. Heal. Monit.* 10(6):631–642.
[293] Wulandhari LA, Wibowo A, Desa MI (2015) Condition diagnosis of multiple bearings using adaptive operator probabilities in genetic algorithms and back propagation neural networks. *Neural Comput. Appl.* 26(1):57–65.
[294] Luo H, Qiu H, Ghanime G, Hirz M, van der Merwe G (2010) Synthesized synchronous sampling technique for differential bearing damage detection. *J. Eng. gas turbines power* 132(7).
[295] Hoshi T (2006) Damage monitoring of ball bearing. *CIRP Ann. - Manuf. Technol.* 55 (1):427–430. https://doi.org/10.1016/S0007-8506(07)60451-X.
[296] Saravanan S, Yadava GS, Rao PV (2006) Condition monitoring studies on spindle bearing of a lathe. *Int. J. Adv. Manuf. Technol.* 28(9−10):993–1005.
[297] Huang Y-C, Shin Y-C (2012) Method of intelligent fault diagnosis of preload loss for single nut ball screws through the sensed vibration signals. *Int. J. Mech. Mechatronics Eng.* 6(5):1022–1029.
[298] Niu L, Cao H, He Z (2014) Dynamic modeling and vibration response simulation for rolling ball bearings with local surface defects. *Zhendong Ceshi Yu Zhenduan/Journal Vib. Meas. Diagnosis* 34(2):356–360.
[299] Li Y, Cao H, Chen X (2015) Modelling and vibration analysis of machine tool spindle system with bearing defects. *Int. J. Mechatronics Manuf. Syst.* 8(1−2):33–48.
[300] Tan J, et al. (2009) Study of frequency-shifted and re-scaling stochastic resonance and its application to fault diagnosis. *Mech. Syst. Signal Process.* 23 (3):811–822.
[301] Tu JF (1996) Strain field analysis and sensor design for monitoring machine tool spindle bearing force. *Int. J. Mach. Tools Manuf.* 36(2):203–216.
[302] DEmilia G, Gaspari A, Hohwieler E, Laghmouchi A, Uhlmann E (2018) Improvement of defect detectability in machine tools using sensor-based condition monitoring applications. *Procedia CIRP* 67:325–331.
[303] Möhring H-C, Bertram O (2012) Integrated autonomous monitoring of ball screw drives. *CIRP Ann* 61(1):355–358.
[304] Li K, et al. (2020) Vibration-based health monitoring of ball screw in changing operational conditions. *J. Manuf. Process.* 53:55–68.
[305] Jia P, Rong Y, Huang Y (2019) Condition monitoring of the feed drive system of a machine tool based on long-term operational modal analysis. *Int. J. Mach. Tools Manuf.* 146:103454.
[306] Verl A, Heisel U, Walther M, Maier D (2009) Sensorless automated condition monitoring for the control of the predictive maintenance of machine tools. *CIRP Ann* 58(1):375–378.
[307] Nguyen TL, Ro S-K, Park J-K (2019) Study of ball screw system preload monitoring during operation based on the motor current and screw-nut vibration. *Mech. Syst. Signal Process.* 131:18–32.